Long-Range Forecasting and Climate Research

The climate of the world

IV — Climate change: the ancient earth to the 'Little Ice Age'

by

C.K. Folland

LRFC 4 March 1986

LONG RANGE FORECASTING AND
CLIMATE RESEARCH MEMORANDUM NO. 4
(LRFC 4)

THE CLIMATE OF THE WORLD

IV - CLIMATIC CHANGE: THE ANCIENT EARTH TO THE "LITTLE ICE AGE"

by

C K FOLLAND

BASE ON TWO ADVANCED LECTURES DELIVERED
TO THE SCIENTIFIC OFFICERS' COURSE,
METEOROLOGICAL OFFICE COLLEGE, MARCH 1985

Met O 13 (Synoptic Climatology Branch)
Meteorological Office
London Road
Bracknell
Berkshire RG12 2SZ

March 1986

This Memorandum is the fourth in a series of six on:

THE CLIMATE OF THE WORLD

BY

C K Folland and D E Parker

Based on nine Advanced Lectures delivered by C K Folland to the Scientific Officers' Course, 1-7 March 1985, and one Advanced Lecture delivered by D J Carson in March 1982.

INDEX TO SERIES

ADVANCED LECTURE NO 6

CLIMATES OF THE PAST I - FROM THE EARLY EARTH TO THE PLEISTOCENE ICE AGES

6.1 Summary

Lectures 6-8 are concerned with the history of the Earth's climate. The key reference is Lamb (1977). The subject is vast and I shall concentrate on selected aspects which are either particularly interesting or where our knowledge is most secure. The standards of proof for past climates can never be as high as for today's climate and many of the deductions depend on bringing together disparate strands of evidence, bound together sometimes by a measure of circular argument. The recent, limited, use of AGCM's to study specific aspects of past climates has tended to support recent empirical reconstructions; so the joint use of observations and models points the way to improvements in our understanding of the remarkable changes of climate that have occurred during the long history of the earth.

6.2 Introduction and the Faint Sun paradox

The further one goes back into the past, the more fragmented the evidence for past climates becomes and it is difficult to establish whether the evidence for a particular climatic feature is really synchronous in time.

Fig 6.1, from Lamb, shows characteristic time-scales over which some influences on climate operate. The first major difficulty one meets is that of solar variability. Astronomers are convinced from theory and observation of other stars that solar luminosity L has increased in the way shown in Fig 6.2. The age of the sun is placed near 4.7 billion years (b.y.) and the age of the earth at 4.5-4.65 b.y. An increase of solar constant, Q, of about 15% since the first recorded ice-age at 2,200 m.y. (million years ago) is embarassingly large. Fig 13, Appendix I to this set of lectures (with Lecture 9), which is derived from an energy-balance model, suggests that the early Earth should have been covered in ice and should not yet have escaped this fate(?). Compensating mechanisms that would increase the past surface temperature include a changed composition of the Earth's atmosphere ie less oxygen and much more carbon dioxide. A much increased transport of heat from equator to pole or an increased flux of geothermal heat would presumably provide less favourable conditions in high latitudes for the onset of glaciation. The latter possibility is not now thought to be significant.

Endal and Schatten (1982) used a simple energy-balance climate model due to North (See Appendix I to this set of lectures) to see if an ice-covered earth having today's atmospheric composition could be avoided if they increased a parameter D that is used in North's model to represent eddy diffusion of heat across latitude circles. Fig 6.3 shows some results which have some complex features; X_s is the sine of the latitude of the ice edge in both hemispheres. Concentrating on D = infinity, an ice-free earth ie $X_s = 1.0$ is just possible for $Q/Q_0 = 0.81$ (Q_0 = today's solar constant). The slope of the line $D = \infty$, (and adjacent lines), is negative so once ice forms, the model solution jumps to a completely ice-covered earth. The addition of an atmospheric greenhouse effect would obviously help to increase temperature but would have to be (a) very large 2,000 million years ago (b) have declined since that time at a rather precise rate to have avoided a later "white" earth catastrophe.

6.3 Evidence for climate of the Earth 2500-200 m.y.

Fig 6.4, taken from Lamb lists the geological eras, their divisions into periods and their sub-divisions into epochs. Fig 6.4 also summarises some opinions about past climates. Fig 6.5 gives a simpler summary of the likely times of ice-age cycles.

6.3.1 Dating ancient rocks - how do we know when geological features were formed?

Dating past rock formations is complex and a main preoccupation of geology. In the ancient past, the relative ages of rocks can be estimated by studying the order in which they were laid down (stratigraphy). Absolute dating requires measurements of the proportions of various radio-active isotopes existing in the rocks, so that use of a specific method would depend on whether a given chemical element exists in the rock. Two examples are given:-

(1) The decay of the radio active isotope of potassium ^{40}K to ^{40}A has a half-life of 1.3×10^9 years. So measurements of the amount of argon gas trapped in the rock expressed as a ratio of the amount of ^{40}K still remaining can be used to date some ancient rocks. Extremely old rocks can sometimes be dated using the decay of ^{87}Rb to ^{87}Sr (the rubidium-strontium method); the half-life of this decay is very long: 53×10^9 years. For details of other methods and references see Lamb, pp 70-72.

6.3.2 Earliest evidence of past climate

The first half of the Earth's history has left rather little evidence in its rocks but the second half is increasingly rich in indications of past conditions. For most of the Earth's more recent history the climates have been warmer than now but there is much evidence that from time to time the climate has cooled, at least in some parts of the world. The earliest record of glaciation is that of the Huronian of about 2250 million years ago (Harland and Herod (1975)) discovered in the USA in the region of Lake Huron. There is little evidence of glaciation in the next 1000 million years but the Precambrian period of 950-650 million years ago produces evidence of (perhaps) three widespread glaciations down to quite low latitudes.

Harland and Herod (1975) discuss the Precambrian glaciations but it is difficult to make reliable deductions, as the relative proportions and extent of the continents at that time are not well known. However, Harland and Herod believe that the Precambrian ice-sheets have at least approached the equator so there is a possibility that a close approach (surely not reached!) to a "white" Earth occurred at that time.

6.3.3 Cambrian (500 m.y.) to Permian (200 m.y.) times

Understanding of this period of Earth's history has been revolutionised in the last few decades by the ideas of continental drift and plate tectonics. A lively account is given by Tarling and Tarling (1974). Some details remain controversial, but the crucial step that converted speculations about the meaning of remarkable geometrical fits between various continents (especially if their shapes were measured near the edges of the continental shelves) into an almost universally accepted theory of continental drift involved the measurement of remanent palaeomagnetism in ancient rocks. When rocks containing iron cool, they retain a remanent magnetism that reflects the local earth's magnetic field at that time (ie the angle of dip, magnetic north vector etc). From time to time, geologically very sudden changes in the direction of the remanent magnetic field occur, usually by 180°. This indicates a recurring total reversal of earth's magnetic field. These reversals can be followed in many continental rocks; The last reversal occurred about 730000 years ago. Even more convincingly, these ancient magnetic fields are preserved with great clarity in the basaltic ocean floors as a series of magnetic stripes so that each stripe is reversed in polarity by 180° with respect to adjacent stripes. These observations indicate that the ocean floor is continually being formed by spreading out from the observed volcanically active (submerged) mid-ocean ridges. The convective cells in the Earth's mantle that caused the sea-floor spreading also provide the energy to move the continents or at least individual continental blocks known as "plates". So it is possible to fix the latitudes of the plates in ancient times by measuring the remanent palaeomagnetic vectors using a magnetometer, and by assuming that Earth's magnetic poles were always near the geographical pole.

Fig 6.6(A) and (B) give reconstructions of the continents 500 m.y., 340 m.y., 250 m.y. and 50 m.y. as illustrated by Lamb. The changing positions of the continents are likely to affect climate:-

(a) Locally, as the latitude of a given location changes eg Fig 6.6 shows that England both "existed" and was probably near 15°S at 340 m.y., 15°N at 250 m.y. and 40°N at 50 m.y.

(b) Because the global proportion of land in higher and lower latitudes progressively changes.

(c) As a result, the meridional heat flux (equivalent to D in Fig 6.3) should change with the changing ocean currents and atmospheric circulation.

Fig 6.7, taken from Sellers and Meadows (1975), shows how the broad pattern of ice ages shown in Fig 6.5 is reflected in variations in the fraction of latitudes higher than 60°N or 60°S estimated to have been occupied by land. So a large land surface may be required in high latitudes whose albedo can be increased by snow and eventually by ice but some mechanism for delivering large quantities of precipitation to these surfaces over long periods would also be needed.

Figs 6.8 and 6.9 show two reconstructions of past glaciations:-

(a) Ordovician times (about 400 m.y.)

(b) In Permo-carboniferous times (about 250 m.y.)

The Ordovician ice age affected the Sahara (Fig 6.8) and parts of S America. Before the widespread acceptance of continental drift, this glaciation posed a severe problems to climatologists who had to invent a climate with both an equatorial ice cap and no high latitude ice caps. Brooks (1949) proposed an elaborate theory of a world containing an ice cap in equatorial regions only. The evidence for the Ordovician ice age is strong, with eroded but recognisable geological features which are widespread in parts of the dry Sahara eg in the Tibesti Mountains; the remnants include U-shaped valleys, glacial morains etc. The subsequent Permo-carboniferous ice age affected Antarctica, Australia and S India. In fact Antarctica has probably remained quite close to the S Pole since that time (Fig 6.6) and given the difficulty of obtaining evidence from Antarctica, it is not absolutely clear whether deglaciation has ever been complete since Permo-Carboniferious times. Finally both glacial periods show signs of interglacials, as in the recent ice age, but the geological evidence is only capable of showing gross fluctuations.

6.3.4 Cosmic theories of ice ages

The apparent rhythmic nature of the 3 or 4 Ice Age epochs since the late Precambrian has prompted theories about their possible cosmic origins. Cosmic factors would now be regarded as additional to those involving continental drift.

One theory due to Urey (see Opik (1965)) suggests that the sun varies in its radiation output as it goes round the galactic centre. This would produce variations on time scales of 250 million years. Another theory (due to McCrae),which would produce solar radiation variations on the same time-scale, concerns the fact that as the solar system orbits the centre of our galaxy, it passes through galactic dust clouds which reduce the solar constant (Opik (1965)). We are currently in a glacial period and these dust clouds are not now evident so the theory seems to assume that the most recent ice age epoch has finished.

6.4 The Mesozoic and Cenozoic Eras, excluding the Pleistocene Epoch (200-3 m.y.)

6.4.1 Mesozoic era

This era was the heyday of the dinosaurs. Fig 6.6 indicates that both Poles were open or virtually open to the global ocean circulation and no evidence of glaciation has yet been found but considerable evidence of warm climates has been found. This is a period when limestone rocks were laid down, many of which show a banded structure with depth; evidence has started to accumulate that these structures are associated with Milankovitch radiation variations but this idea is very recent and on the face of it puzzling in the absence of a glaciation-deglaciation cycle. Interested readers should refer to the two volumes on "Milankovitch and Climate" published in 1984 which are referenced later in this lecture. The latter part of this period is mysterious; quite suddenly the dinosaurs and many other animals died out in what appeared to be mass extinctions. There is accumulating geological evidence of a volcanic or meteoric "glassy" layer in the rocks in several parts of the world dated at about 65 m.y. So it is possible that massive volcanism or an impact with a giant meteorite may have occured, perhaps causing mass extinctions via catastrophic short-term reduction of insolation. If so, the climate did not change for long enough for the evidence to have survived, and no ice-age resulted.

6.4.2 Cenozoic Era - Tertiary period

The Tertiary provides the first quantitative evidence for the values of ocean temperatures. The main tool is the measurement of the quantity of the isotope of oxygen ^{18}O in marine foraminifera, which are types of plankton whose ancient shells are found on the ocean bed. Annex I to this lecture describes the oxygen isotope method of measuring palaeo-temperatures. The shells are made of calcium carbonate and Fig 6.10 shows an example: the species globorotalia menardii. We shall discuss these types of measurement in the next section, but remark here that the ^{18}O method requires measurement of the ratio of $^{18}O/^{16}O$ in the calcarious shells of the foraminifera. Unfortunately, this ratio depends not only on ocean temperature but also on whether the oxygen isotope ratio in the oceans themselves changes. Such changes would occur if glaciers formed on land when the concentration of ^{18}O would rise in the oceans as the glaciers developed.

Over the last 30 years the USA Deep-Sea Drilling Project has provided many deep-sea sedimentary cores containing these shells. Because the length of the cores that can be extracted from the ocean bed is currently limited to about 20 m, areas of the deep ocean which have a very low sedimentation rate are required for measuring temperature profiles through the long time interval encompassed by the Tertiary. Dating of these cores can sometimes be done using the magnetic reversals mentioned before. In addition, the relative proportions of different planktonic species in the sediments and whether certain species are present or not can be used as a guide to past sea temperatures. However this gets more difficult in the Tertiary as some species have changed since that time. The sea temperatures which the planktonic shells represent depend of course on the depth at which the plankton lived. Some lived near the surface but other forms lived at great depths and these must be correctly identified. Fig 6.11 is a generalised picture of the variation of Tertiary worldwide tropical ocean temperatures deduced by several workers from such cores. This interpretation has been challenged (Matthews and Poore (1980)) and alternative explanations of these measurements include a period of low tropical SST with no ice or a period of high tropical SST with a considerable amount of land ice. Fig 6.12 shows other evidence of climate variations through the Tertiary which suggests a gradual reduction in temperatures towards the present. About 30 m.y., Antarctica and S America drifted far enough apart so that the Drake Passage between them opened up sufficiently for a free flow of ocean water. This is thought to have changed the ocean circulation and helped give rise to a gradual reduction in ocean bottom water temperatures. There is considerable evidence of glaciation in Antarctica from about 17 m.y. (Frakes (1978)) and it is thought that Antarctica has remained partially or wholly glaciated since that time.

6.5 The Quaternary (Pleistocene) Ice Ages (from about 3 m.y.-15000 BP)

Imbrie and Imbrie (1979) contains an easy-to-read account of the history of the evidence and ideas about the Ice Ages. In the last decade there have been two major developments in ideas:-

(1) Evidence is now strong that the ice age/Interglacial oscillations have been almost regular on a 100000 year time scale for the last 800 k.y. and possibly for considerably longer. This regularity has been shown to be related to the Milankovitch radiation variations discussed in Lecture 3. So theories that require random internal variations of the climate system to be the prime initiators of ice ages do not seem to be correct, even if "random changes" play a subsidiary role.

(2) Recent calculations using GCM's suggest that Milankovitch radiation variations are of sufficient size to strongly affect the integrations. However it has not yet been possible to work out the causes of the formation and destruction of the ice age continental ice sheets in any detail, though a number of "simple" models of ice sheets have been constructed, giving a variety of results.

So although many influences have undoubtedly been at work, the Milankovitch radiation variations can probably be regarded as the "pace-makers" of the ice ages. The evidence for this contention will be briefly reviewed, one or two major difficulties highlighted and a couple of GCM integrations carried out for Ice Age radiation conditions are discussed that sum up the problems and prospects.

6.5.1 Empirical evidence for Milankovitch effects

6.5.1.1 The Wrong Evidence

Until fairly recently, a major problem was that crucial observational evidence concerning the timing of past ice ages was wrongly interpreted (Imbrie and Imbrie (1979)). Fig 6.13 shows a diagram of the four Pleistocene ice ages which you may have heard about at school - the Mindel, Riss, Gunz and Wurm ice ages which were worked out by Penck and Bruckner early this century (Imbrie (1982)). It has recently been shown that, except for the Wurm ice age, the other ice ages simply did not exist. The timing of the Wurm ice age was roughly coincident with what is now known to have been the timing of the last glacial maximum but this is regarded as Imbrie as an accident! The four glaciations were derived by Penck and Bruckner from a study of glacial deposits in the Alps; not only have the dates ascribed to the earlier glacial deposits been shown to be incorrect, but the stratification of these glacial deposits has been shown, apparently, to result from tectonic movements and has had nothing to do with climate change at all!.

6.5.1.2 A breakthrough

The initial breakthrough probably came in 1973 when Shackleton and Opdyke (1973), following pioneering work by Emiliani (see Imbrie and Imbrie (1979) for references), produced convincing estimates of the fluctuating volume of ice on the global continents over much of the last million years. This evidence was deduced from a study of plankton shells in a deep sea core in the equatorial Pacific using the oxygen isotope method. (Please see Annex I for a description of the oxygen isotope method). Absolute dating of deep sea cores is difficult unless palaeo-magnetic field reversals can be detected. Shackleton and Opdyke chose a core which could provide detail on much less than a 10,000 year timescale but which nevertheless extended beyond the most recent known magnetic field reversal horizon, known as the Brunhes-Matuyama magnetic reversal. This reversal is now dated at about 730,000 k.y., and its detection in the core allowed the age of different sections of the core to be fixed reasonably well. It is known that deep-ocean sedimentation rates vary in time and cores can be compressed at depth; so this core by itself did not provide an absolute age for most of the temperature variations deduced from the oxygen isotope method. However, it turned out that the relative ages could be deduced quite well given the one measurement of absolute age described above as sedimentation rates do not vary greatly (see Fig 6.14). In Fig 6.14 the ups and downs in $\delta\,^{18}O$ should be (mainly) a record of the changes of ice volume; thus less negative values of $\delta\,^{18}O$ correspond to more ice and/or lower sea temperature. Seven quasi-regular major peaks and troughs can be seen with superimposed higher frequency fluctuations. This (and previous cores from other locations) suggested that seven ice ages occurred at roughly equal intervals back to 73 0000 k.y. because the record of $\delta\,^{18}O$ from any one core should be mainly a record of variations in the worldwide volume of ice on land. It was found possible to match this long core to many previously analysed, shorter, cores obtained elsewhere in the ocean and it began to seem that major ice ages tended to recur at almost fixed intervals of 100,000 years.

Spectral analysis of the core in figure 6.14 suggested strongly that periods of roughly 41,000 and about 22,000 years were present in addition to a 100,000 year peak; these time scales correspond to those of variations in "Milankovitch" northern and southern hemisphere seasonal radiation as described in Lecture 3, shown now in spectral form for several latitudes and months in Fig 6.15. Fig 6.16 shows a later deep sea core (using similar analytic methods) that seemed to support Shackleton and Opdyke's results, together with its spectrum. (See Imbrie and Imbrie (1979) for more details). Lecture 3 showed some of the solar insolation variations as recalculated by Berger and Pestiaux (1984); please refer there. A puzzle however was that no spectral peak of 100,000 years exists in the Milankovitch radiation variations, even though this time scale is dominant in the cores. Nevertheless the amplitudes of the higher frequency seasonal radiation peaks are modulated on the 100,000 year time scale by variations in the eccentricity of earth's orbit, though by a very variable amount.

6.5.1.3 Strong Confirmation of the Ice-Age/Milankovitch radiation variation Link

In 1982, Imbrie et al presented a key paper at a special conference held in USA to debate the Milankovitch radiation variations and their effect on climate. This paper brings together the five most reliably analysed deep-sea ocean cores and their $\delta\,^{18}O$ records, three of which are long enough to reach the Brunhes-Matuyama magnetic reversal (Imbrie et al (1984)). The locations of these cores are shown in Fig 6.17, while Fig 6.18 shows the $\delta\,^{18}O$ data filtered on the obliquity (41,000 year) (curve A) and precession (19000 -23000 year) (curve B) time scales separately, together with similar curves for the amplitude and phase of the astronomical variations of obliquity and precession. Both pairs of curves are normalised to the same vertical scale and small, constant, offsets between the astronomical and $\delta\ ^{18}O$ curves have been removed. The match in amplitude and phase between the $\delta\ ^{18}O$ and astronomical curves is striking as this type of test is quite a sensitive one. However it must be pointed out that this excellent match does reflect several artificial adjustments to the data which chiefly affect the phase match. It is still difficult to explain the dominant 10^5 year cycle in the deep sea cores in terms of the Milankovitch radiation variations, as the 10^5 year amplitude modulation of the shorter time scale radiation fluctuations is far from consistent in magnitude. Many tentative explanations have been given of this cycle relating to the dynamics of ice-sheets and the time it takes for the sheets to form and to melt. Another factor is that when ice sheets form, the rocks beneath sink and when the ice sheets melt it can take a long time for the rocks to rebound. So, if for example, an extensive area of land above a certain altitude in a critical geographical situation was required for glaciation to start during a summer radiation minimum, it could take many thousands of years after the ending of a previous glacial period before this altitude was again reached. At the moment ideas are changing about the time scales involved in the recovery of isostatically depressed rocks (Peltier and Hyde (1984)). These could be longer than hitherto supposed for large areas of millions of km^2 occupied by say the N American ice sheet, roughly coincident with the Laurentian shield area of Canada, including Hudson's Bay.

6.6 Conditions at the glacial maximum

(We shall use "BP" = "Before present" to measure the time elapsed since past ages here).

An interdisciplinary project called CLIMAP (Climate Long-Range Investigation Mapping and Predictions) has attempted to reconstruct the geography of the Ice Age ice sheets and the values of surface ocean temperatures for each month of the year for about 18,000 BP CLIMAP (1981). Evidence was derived from land geology measurements of $\delta\ ^{18}O$, and most importantly, the distribution of species of surface-dwelling plankton found in deep-sea cores which were used as palaeo-thermometers. If we know the current distribution of different kinds of plankton and can relate these to variations of sea temperature, then for a period as recent as 18,000 BP for which evolution of species is not a problem, we can reconstruct past distributions of SST. A complex, multivariate analysis scheme was used to estimate worldwide calendar monthly ocean temperatures. Fig 6.19 shows the reconstructed global SST, together with the extent of the land and ocean ice sheets for August 18,000 BP. Fig 6.20 shows, for the North Atlantic, an estimate of the change of SST from modern values; this ocean cooled the most. See Imbrie and Imbrie (1979) for further details and other references.

.7 Numerical model experiments

6.7.1 Manabe and Broccoli (1984) (MB)

MB used a coupled mixed ocean-layer spectral AGCM. They set out to determine what the physical effects of the land ice sheets existing at 18,000 BP on SST might be. The model was integrated for 20 model years and the last 5 years of the integrations averaged. So all months of the year were modelled.

(a) Control experiment

Modern continental ice extent, today's radiation conditions.

(b) Anomaly experiment

CLIMAP continental ice extent, today's radiation conditions (at 18000 BP the radiation conditions happened to be similar to today's, as the ice age summer radiation minimum and winter radiation maximum in the N Hemisphere occurred several thousand years previous to this time).

Fig 6.21 shows the SST difference between anomaly and control experiments and also the difference in February and in August between the SST values reconstructed by CLIMAP for 18,000 BP and today's values. In the N Hemisphere, SST's in the anomaly experiment are much lower in both months in the N Atlantic and N Pacific, and these changes agree quite well with the CLIMAP reconstructions. In the S Hemisphere the differences in SST between anomaly and control experiments are mostly positive so that S Hemisphere SST was mostly warmer in the anomaly experiment, ie at 18000 BP. The CLIMAP reconstruction shows that some areas in the S Hemisphere were warmer but many areas were substantially colder than now. The model results suggest, therefore, that the presence of the N Hemisphere ice sheet may have little effect on SST in the S Hemisphere. The reason (in the model) appears to be that although the S Hemisphere reflected more incoming solar radiation at 18,000 BP, this was almost exactly compensated by a lower emission rate of long wave radiation. So an insignificant change in net hemispheric heat exchange occurred to balance the difference in heating. Thus some other mechanism may be needed to provide the observed cooling of the S Hemisphere. MB suggest that recent measurements (see Lecture 9) which show a lower concentration of carbon dioxide in the atmosphere at that time might provide the missing physical link. It is still something of a puzzle as to why both hemispheres suffered glaciation at the same time; radiation was of course near a maximum in the southern summer at this time, rather like now.

6.7.2 Royer et al (1984)

Royer et al used a numerical model to study the annual cycle of climate at 125,000 BP when N Hemisphere radiation was at a maximum and at 115,000 BP when N Hemisphere radiation was at a minimum. The earlier date coincided with the last interglacial, rather like the present one, now known as the Eemian interglacial. The orbit of the earth was highly eccentric at both times (e = 0.05) so an especially large change in N Hemisphere summer radiation occurred between these two dates. The experiment was rather short, the model being integrated only through one annual cycle. In both cases the modern distribution of land ice and modern values of SST were assumed. We shall highlight only one aspect of the results - does the model provide evidence that ice might preferentially form in eastern Canada in 115000 BP where the largest of the continental ice sheets in fact developed in recent Ice Ages? (Fig 6.19 shows the ice extent at height of the last ice age). Fig 6.22 shows the difference in simulated annual mean surface temperature 115000 BP -125000 BP. The largest cooling in the N Hemisphere at 115000 BP is indeed in eastern Canada. Furthermore model soil water content, which include the effect of snow accumulation, also increased in this region. Fig 6.23 shows the differences in PMSL. It was found that the model maintained colder conditions in most of the year in Eastern Canada partly due to higher pressure in winter at 115,000 BP (despite increased winter radiation) but also due to cloudier summers which of course were accompanied by less solar insolation. So the results of these experiments, although tentative, are encouraging.

ANNEX I TO LECTURE 6

OXYGEN ISOTOPE METHOD FOR DEDUCING GLOBAL ICE VOLUME, OCEAN TEMPERATURE AND AN INDEX OF AIR TEMPERATURE OVER LARGE LAND GLACIERS

A(1) δ in polar ice

Consider the evaporation of water from the ocean surface (Fig 6AI). There are three oxygen isotopes ^{16}O, ^{17}O, ^{18}O, of which ^{17}O can be neglected. The average ratio of the quantity of ^{16}O:^{18}O in today's oceans is 998:2. The saturation vapour pressure of (A) $H_2{}^{18}O$ is less than that of (B) $H_2{}^{16}O$; the ratio $^{A}/_{B}$ = 0.99 at 0°C and 0.992 at 25°C and the difference continues to reduce slowly at higher temperatures. So there is always a lower fraction of ^{18}O in atmospheric water vapour than in the ocean. Now, $H_2{}^{18}O$ vapour preferentially condenses into the liquid or solid form as its saturation vapour pressure is lower than that of $H_2{}^{16}O$. The varying values of the ratio A/B quoted above suggests that condensation will produce relatively more ^{18}O in rain and snow at lower temperatures than at high temperatures. This effect is offset at higher latitudes by (a) the fact that the water in precipitation will have been derived from cooler seas (mainly sub-tropical or mid-latitude) so less ^{18}O is evaporated than in the tropics and (b) most importantly, condensation and precipitation at higher latitudes and altitudes will be from water vapour already further depleted in ^{18}O by preferential condensation and precipitation of $H_2{}^{18}O$ vapour at lower latitudes and lower altitudes. Nevertheless any condensed precipitation will contain at least a little less ^{18}O than the parent ocean water. The process becomes impossibly complex to unravel if precipitation falls on land and is re-evaporated and reprecipitated so measurements of ^{18}O in frozen precipitation on ice sheets only have a (rough) meaning if the precipitated vapour is (mostly) derived directly from the oceans. The amount of ^{18}O is measured by δ:-

$$\delta = 1000\,\frac{(^{18}O/^{16}O\ \text{(sample)} - {}^{18}O/^{16}O\ \text{smow})}{^{18}O/^{16}O\ \text{smow}}$$

smow = standard mean ocean water. In one set of measurements (Dansgaard (1964)) quoted by Lamb (1977); the following was found (δ_p = δ in precipitation:)

At Valentia	δ_p = -6	annual mean surface air temp T_a = 11°C
At Upenowsk (Greenland)	δ_p = -18	" " " " " " = -7°C
At South Pole	δ_p = -49	" " " " " = -49°C

Note that all values are negative because all precipitation will contain at least a little less ^{18}O than is contained in smow (1st paragraph above).

Dansgaard gives a formula relating T_a to δp.

$$0.7\,T_a = \delta_p + 13.6$$

The δ values are preserved in glacier ice and show substantial seasonal variations which are easily detected in some ice samples as δ can be measured with a standard error of about $\pm$ 0.2 considerably less than the seasonal variations. We shall consider measurements of δ in ice sheets in Lecture 7.

A(2) δ in the shells of plankton and global ice volume

Shells made of calcium carbonate in principle contain more ^{18}O than sea water. The equilibrium amount depends on water temperature; the ratio $^{18}O_{SHELL}/^{18}O$ SEA ($^{18}O_s/^{18}O_w$) varies from 1.025 at 0°C to 1.021 at 25°C. So δ_s becomes more positive as sea temperature falls. In practice the δ_s values have a further "constant" offset from calculated equilibrium values by an amount which depends on the specific plankton species (of foraminifera usually) which can cause the δ_s value to be negative but the temperature response will remain the same. An equation often used is

$$T = 16.9 - 4.38\,(\delta_s-\delta_w) - 0.10\,(\delta_s-\delta_w)^2$$

where δ_w is the δ of ambient sea water (relative to smow), when the plankton was alive.

It used to be thought that $\delta_s-\delta_w$ in deep sea cores mostly varied with temperature, ie δ_w did not change much through time eg through the ice ages at a specific location. This is now known not to be true. δ_w rises if large quantities of land ice form as land ice contains less ^{18}O than the ocean, as shown in Section A(1). So the presence of continental ice sheets increases the concentration of ^{18}O in the ocean. The amount of the increase depends mainly on the change in the volume of land ice relative to that of the oceans and, appreciably, on the sea and air temperatures prevailing when the land ice was formed. Observations of δ in ice sheets and in deep sea cores show that δ_w varies considerably more than $\delta_s-\delta_w$, under most conditions. It is then easy to show that δ_s represents the changes through time of δ_w, rather than those of T, ie the changes mainly represent the changes in global ice volume.

So, from δ measurements in ice sheets, δ_s can be calibrated to measure the approximate changes in the volume of worldwide land ice, in km^3 (roughly 1% change of δ per 30 x 10^6 km^3 of ice). However the effect of sea temperature on δ_s is not always negligible, and global ice volume changes can only be monitored semi-quantitatively unless additional geological evidence is at hand. If we assume an ice free world, as some authors do for the Tertiary epoch, quite large changes in sea temperature can be deduced from δ_s measurements which would be exaggerated if land ice volume, in reality, changed appreciably.

REFERENCES TO ADVANCED LECTURE 6

BERGER, A AND PESTIAUX, P (1984) Accuracy and Stability of the Quaternary Terrestrial Insolation. Milankovitch and Climate, Pt I. Ed: A Berger et al, NATO ASI 126, pp 83-111.

BROOKS, C E P (1949) Climate through the ages. Benn, London, Revised Ed.

CLIMAP Project Members (1981). Seasonal Reconstruction of the Earth's surface at the last global maximum. Geological Society of America Map and Chart Series MC-36.

DANSGAARD, W (1964) Stable isotopes in precipitation. Tellus, 16, pp 436-468.

ENDAL, A S AND SCHATTEN, K W (1982) The faint young sun-climate paradox: continental influences. J Geophys Res, 87, C9, pp 7295-7302.

FRAKES, L A (1978) The long-term climatic record: Cenozoic climates: Antarctica and the Southern Ocean. In Climatic Change and Variability - a Southern perspective. Ed: A B Pittock et al. Cambridge Univ Press, pp 53-69.

FRAKES, L A (1979) Climates throughout geologic time. Elsevier.

HARLAND, W B AND HEROD, K N (1975) Glaciations through time. In "Ice Ages Ancient and Modern", pp 189-216. Seel House Press, Liverpool.

HOLMES, A (1965) Principles of Physical Geology (2nd edition). Nelson.

IMBRIE, J (1982) Astronomical theory of the Pleistocene Ice Ages: A brief historical review. Icarus, 50, pp 408-422.

IMBRIE, J; HAYS, J D; MARTINSON, D G; McINTYRE, A; MIX, A C: MORLEY, J J; PISIAS, N G; PRELL, W L AND SHACKLETON, N J (1984) The orbital theory of Pleistocene Climate: Support from a revised chronology of the marine $\delta^{18}O$ record. Milankovitch and Climate, Pt I. Ed: A Berger et al, NATO ASI 126, pp 269-305.

IMBRIE, J AND IMBRIE, K P (1979) Ice Ages - Solving the Mystery. MacMillan, London.

LAMB, H H (1977) Climate: present, past and future Vol 2. Methuen.

MANABE, S AND BROCCOLI, A J (1984) Influence of the CLIMAP ice-sheet on the climate of a general circulation model: implications for the Milankovitch theory. Milankovitch and Climate, Pt II. Ed: A Berger et al, NATO ASI 126, pp 789-799.

MATTHEWS, R K AND POORE, R Z (1980) Tertiary $\delta^{18}O$ record and glacio-eustatic sea-level fluctuations. Geology, 8, pp 501-504.

OPIK, E J (1965) Climatic change in cosmic perspective. Icarus N-Y, 4, pp 289-307.

PELTIER, W R and HYDE, W (1984) A model of the ice age cycle. Milankovitch and Climate, Pt II. Ed: A Berger et al, NATO ASI 126, pp 565-580.

ROYER, J F; DEQUE, M AND PESTIAUX, P (1984) A sensitivity experiment to astronomical forcing with a spectral GCM: simulation of the annual cycle at 125000 BP and 115000 BP. Milankovitch and Climate, Pt II. Ed: A Berger et al, NATO ASI 126, pp 733-764.

SELLERS, A AND MEADOWS, A (1975) Long term variations in the albedo and surface temperature of the earth. Nature, 254, p 44.

SHACKLETON, N J AND OPDYKE, N D (1973) Oxygen isotopic and paleomagnetic stratigraphy of equatorial Pacific core V28-238: oxygen isotope temperatures and ice volume on a 10^5 year and 10^6 year scale. Quaternary Research, 3, pp 39-55.

TARLING, D H AND TARLING, M P (1974) Continental Drift. Penguin Books.

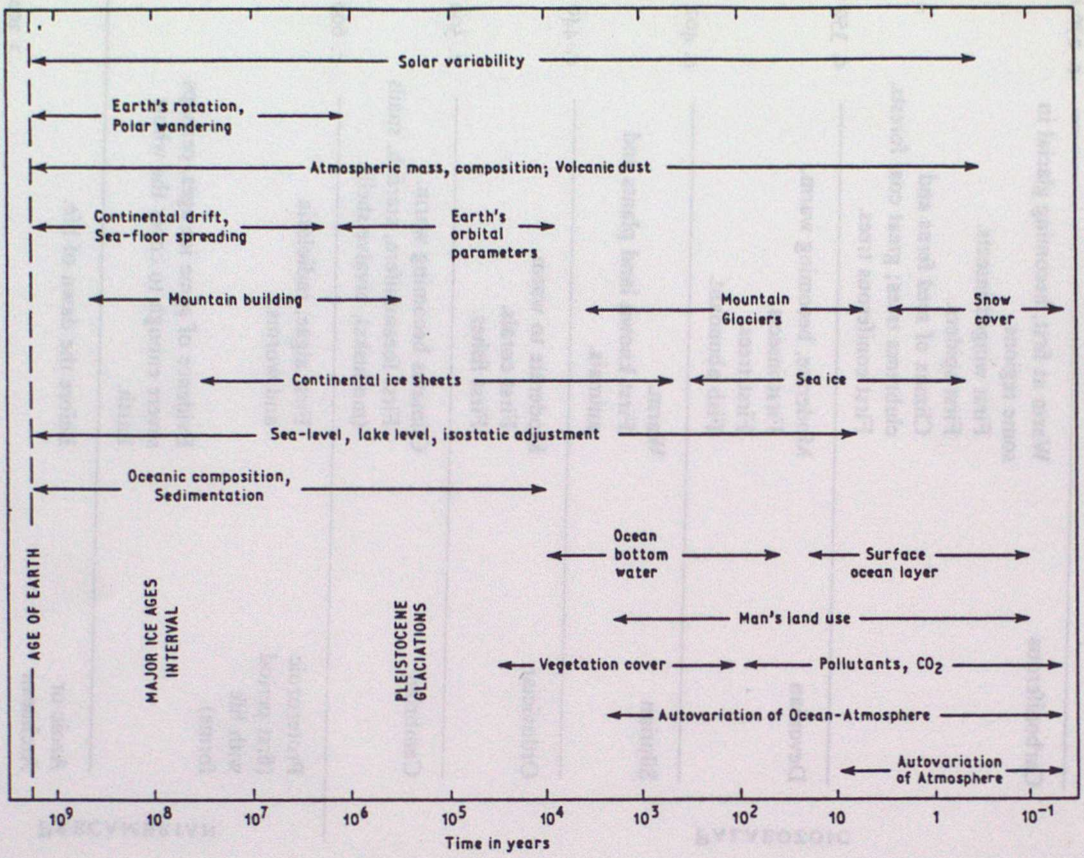

Figure 6.1 Time-scales of influences on climate.
From Lamb (1977)

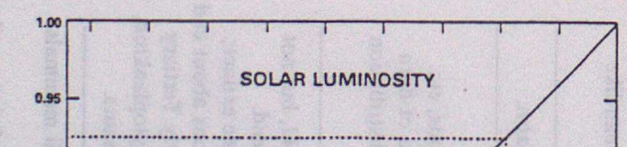

Figure 6.2 Modelled history of solar luminosity (from Endal and Schatten (1982))

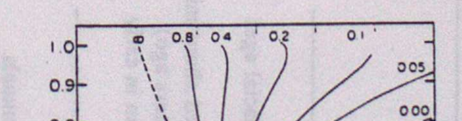

Figure 6.3 Ice-edge latitude versus solar radiation input for models with various values of atmospheric eddy diffusion parameter D. (From Endal and Schatten (1982))

Table App. V.1 Geological eras and their subdivisions, with time scale

Era	System or Period	Series or Epoch	Notes on climate, fauna and flora	Radiometric age
Cenozoic (Kainozoic)	Quaternary	Holocene or Recent (post-glacial)		
				c. 10 000 years ago
		Pleistocene	Glaciations and Interglacial ages alternating. *Homo sapiens* emerged about mid last glacial (40 000 years ago). Earliest forms of Man in early Pleistocene.	
				1–3 million years ago
	Tertiary	Pliocene	Becoming colder. Large carnivorous animals.	
				c. 10 million years ago
		Miocene	Warm to moderate. Whales, apes and grazing animals.	
				c. 25 million years ago
		Oligocene	Warm. First monkeys and man-like apes.	
				c. 40 million years ago
		Eocene	Moderate becoming warm.	
				c. 60 million years ago
		Palaeocene	Becoming warmer. Early horses, elephants, etc. Most modern genera of flora present, but world distribution different.	
				c. 70 million years ago
Mesozoic	Cretaceous		Some evidence of a cold, but not glacial phase towards end. Ichthyosaurus became extinct; many other extinctions about end of Cretaceous to early Tertiary including among phytoplankton, marine turtles, dinosaurs.	
				c. 130 million years ago
	Jurassic		First birds and small mammals. Dinosaurs' heyday. First crocodiles and flying reptiles.	
				c. 180 million years ago
	Triassic		First dionosaurs, ichthyosaurus, etc.	

Table App. V.1 – continued

Era	System or Period	Series or Epoch	Notes on climate, fauna and flora	Radiometric age
				c. 230 million years ago
Palaeozoic	Permian		Glacial at first, later moderate. Conifers abundant.	
				c. 270 million years ago
	Carboniferous		Warm at first, becoming glacial in some regions. First winged insects. First spiders. Climax of seed ferns and clubmoss trees; great coal forests. First coniferous trees.	
				c. 350 million years ago
	Devonian		Moderate, becoming warm. First insects. First trees. Fish abundant.	
				c. 400 million years ago
	Silurian		Warm. First known land plants and animals.	
				c. 440 million years ago
	Ordovician		Moderate to warm. First corals. First fishes.	
				c. 500 million years ago
	Cambrian		Climates becoming warm. First foraminifera, starfish, snails (mollusks), bivalve shells.	
				c. 600 million years ago
Precambrian	Proterozoic (first period with life forms)		First algae, radiolaria and worms. Evidence of some ice ages, perhaps severe enough to cover the whole Earth.	
	Azoic or Archaean		Before the dawn of life.	
				> 3000 million years ago

Figure 6.4 From Lamb (1977)

The Geological Time Scale

(millions of years).

2250 B.P.	Huronian Ice Sheet
950-650 B.P.	Pre-Cambrian Ice Ages
450 B.P.	Ordovician Ice Age
300 B.P.	Permo-Carboniferous Ice Age
50 B.P.	Start of cooling
2 ? B.P.	Start of Quaternary Ice Age

Figure 6.5.

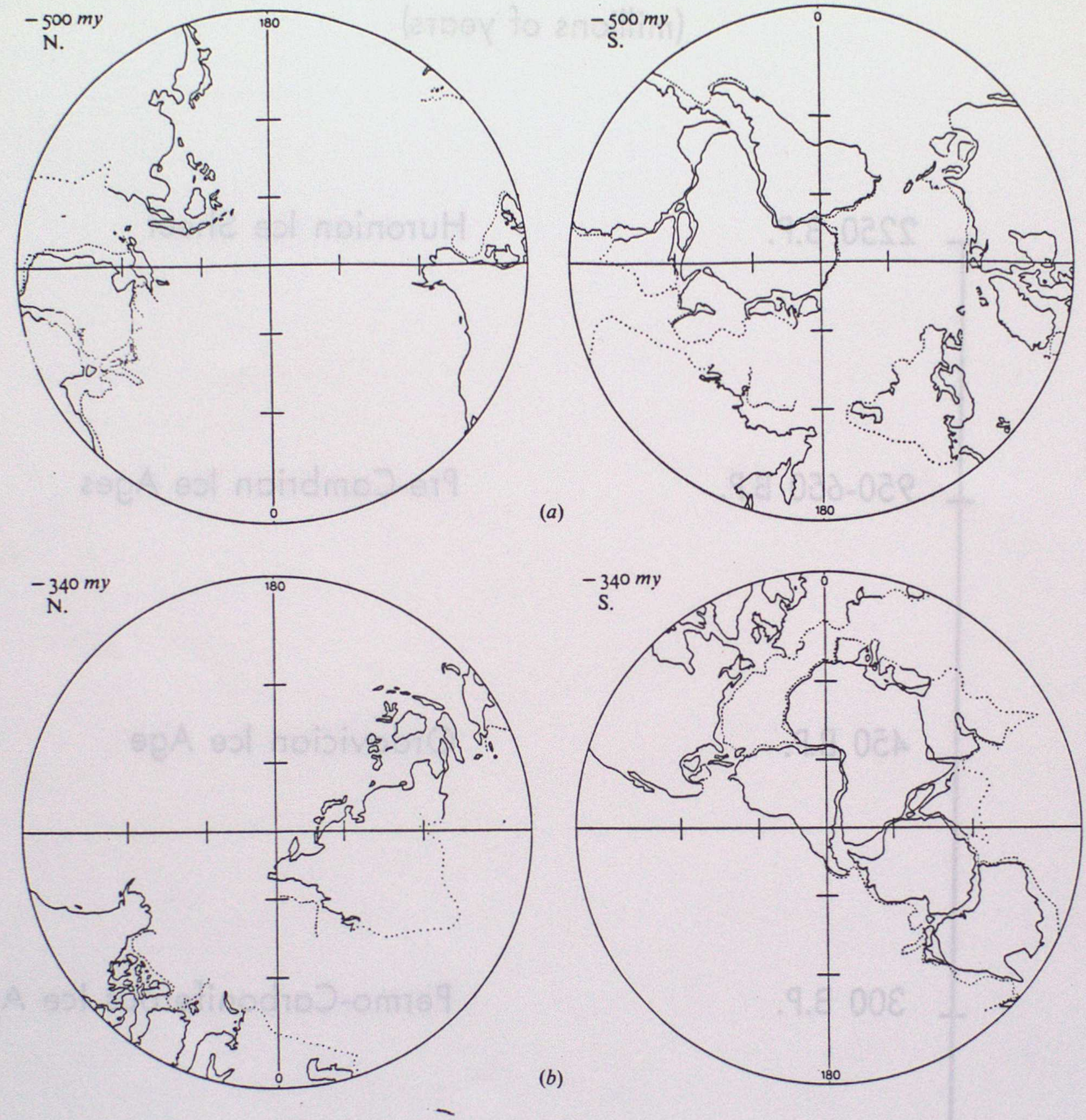

Figure 6.6A Palaeogeographies. From Lamb (1977)

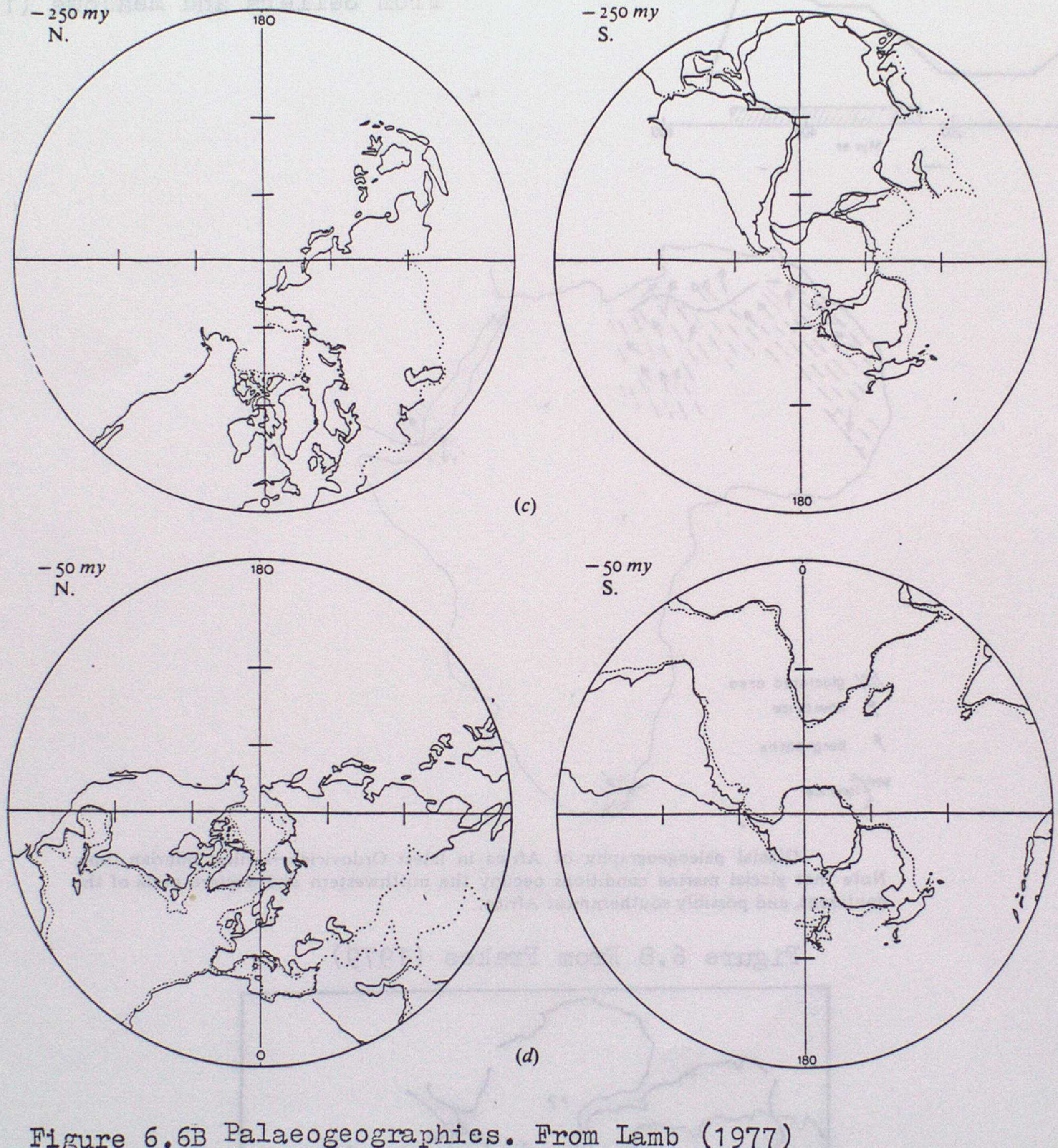

Figure 6.6B Palaeogeographies. From Lamb (1977)

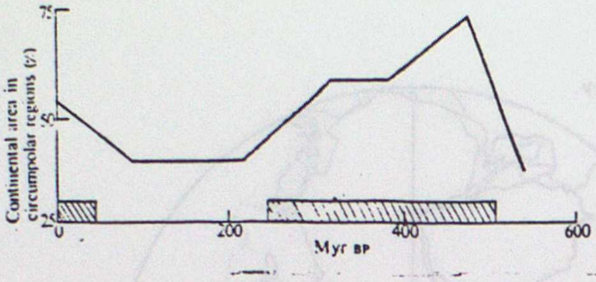

Figure 6.7 History of circumpolar land coverage. From Sellers and Meadows (1975)

Glacial paleogeography of Africa in latest Ordovician—earliest Silurian time. Note that glacial marine conditions occupy the northwestern and western parts of the continent, and possibly southernmost Africa.

Figure 6.8 From Frakes (1979)

Figure 6.9 Permo-Carboniferous glaciations, after Holmes, 1965.

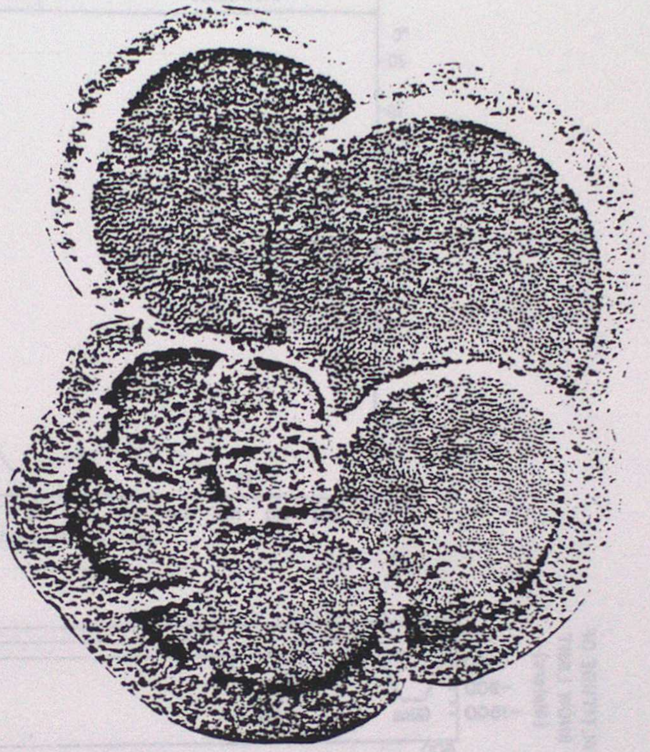

Figure 6.10 Example of shell of marine foraminifera. From Imbrie and Imbrie (1979)

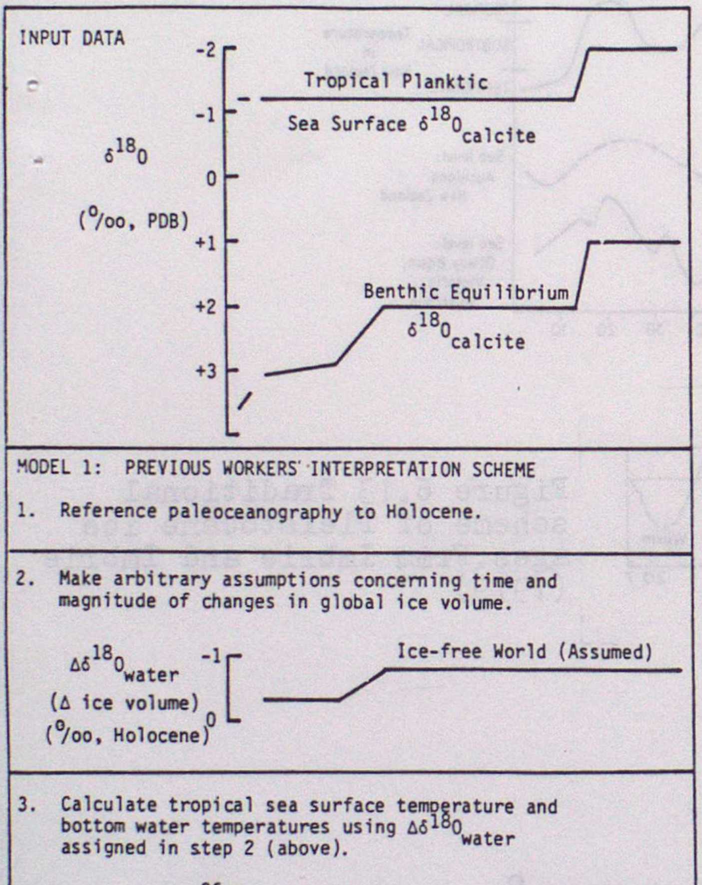

Figure 6.11 Generalised oxygen-18 isotope record and its interpretation. From Matthews and Poore (1980)

Figure 6.12 Temperature in the Tertiary. From Lamb (1977)

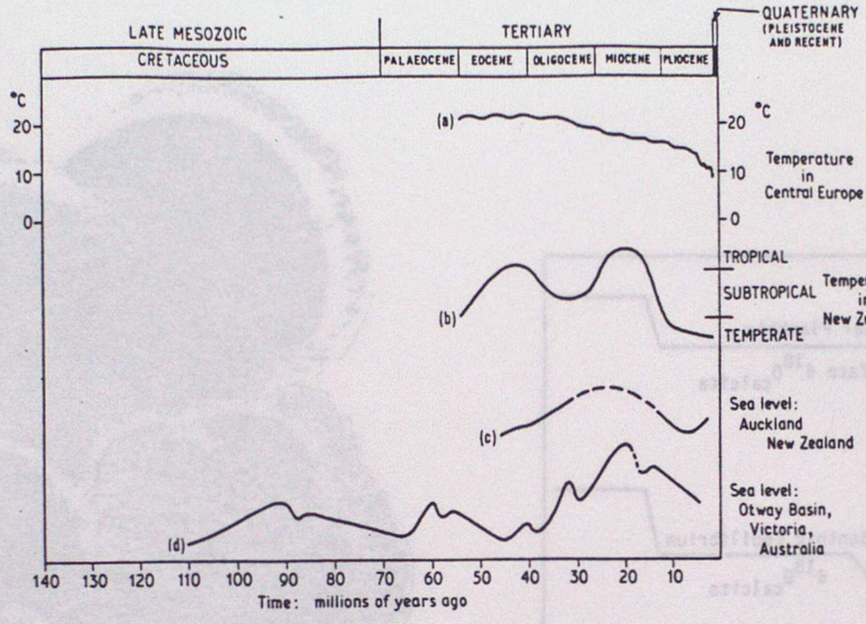

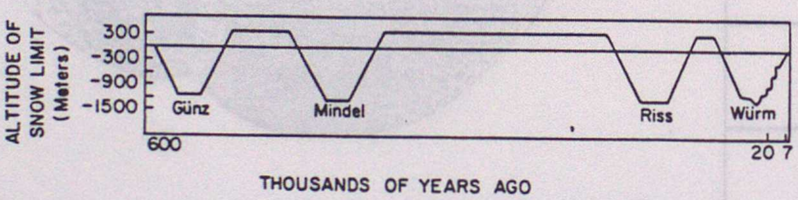

Figure 6.13 Traditional scheme of Pleistocene ice ages. From Imbrie and Imbrie (1979)

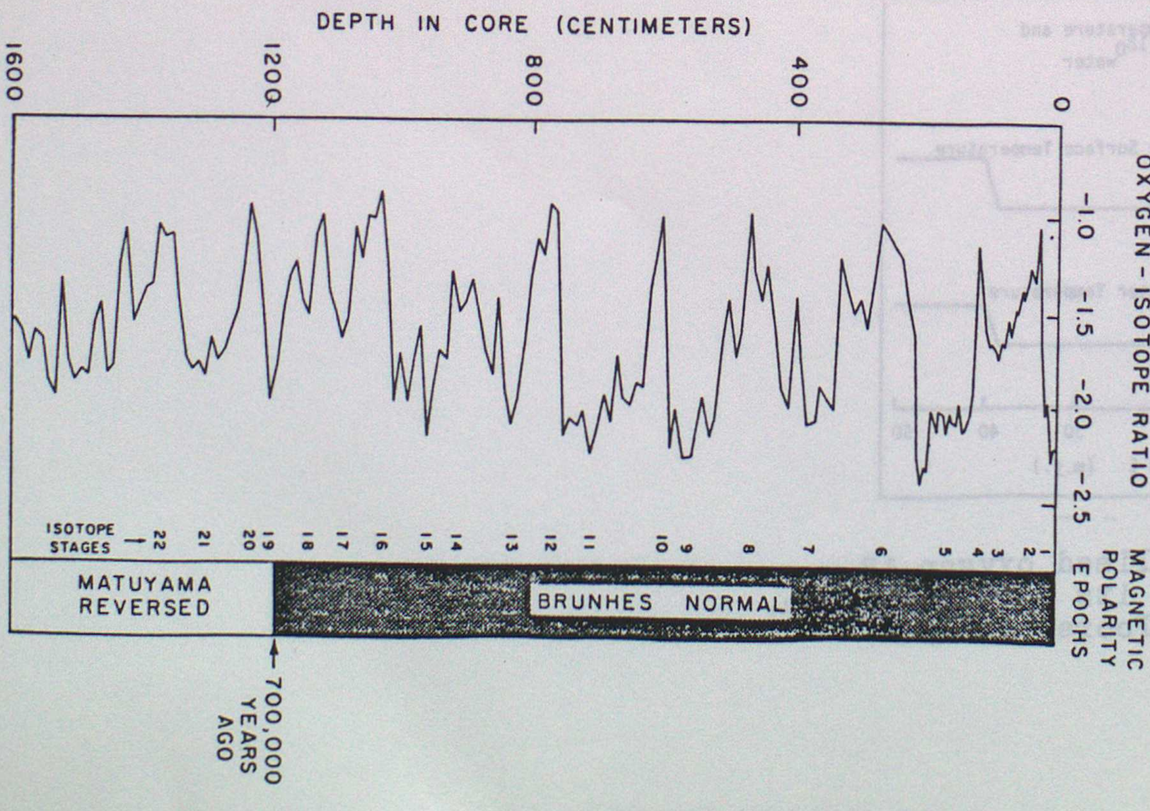

Figure 6.14 Comparison of isotopic and magnetic measurements for the Pleistocene. From Imbrie and Imbrie (1979)

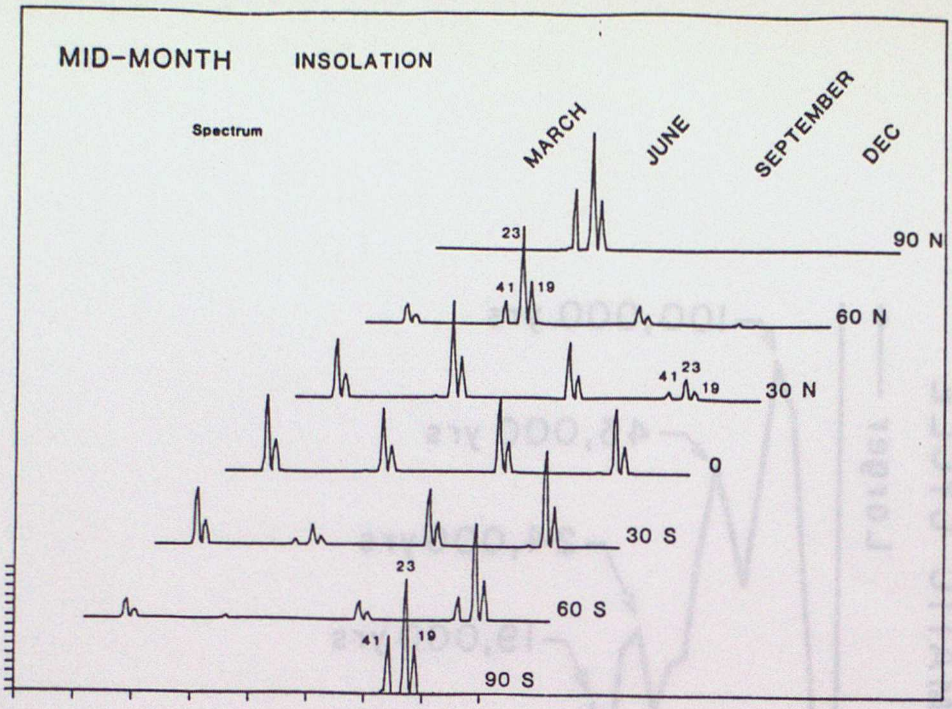

Figure 6.15 Spectral analysis of mid-month insolation. From Berger and Pestiaux (1984).

(Figure 6.16 follows Figure 6.17)

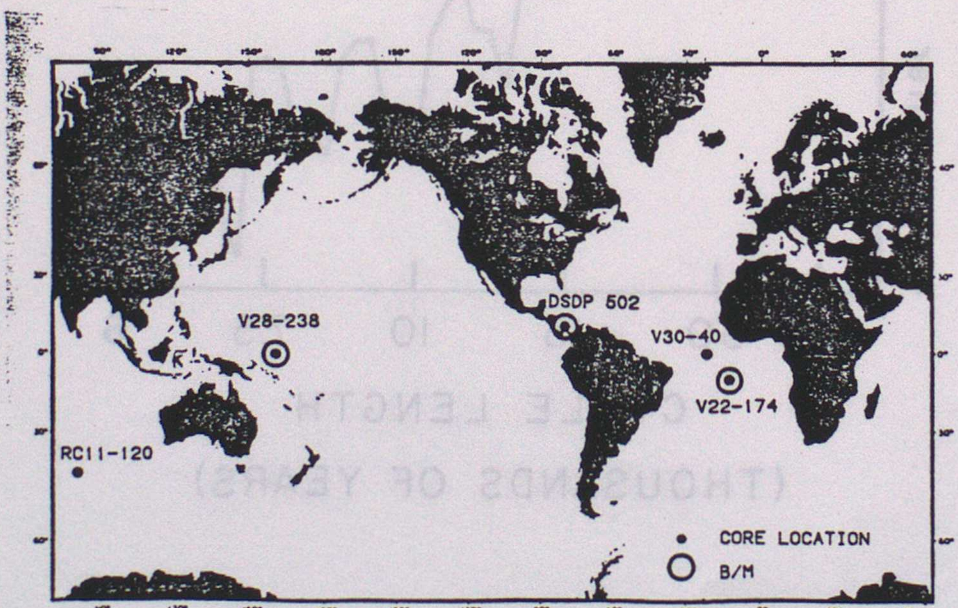

Figure 6.17 Location of cores used by Imbrie et al (1984)

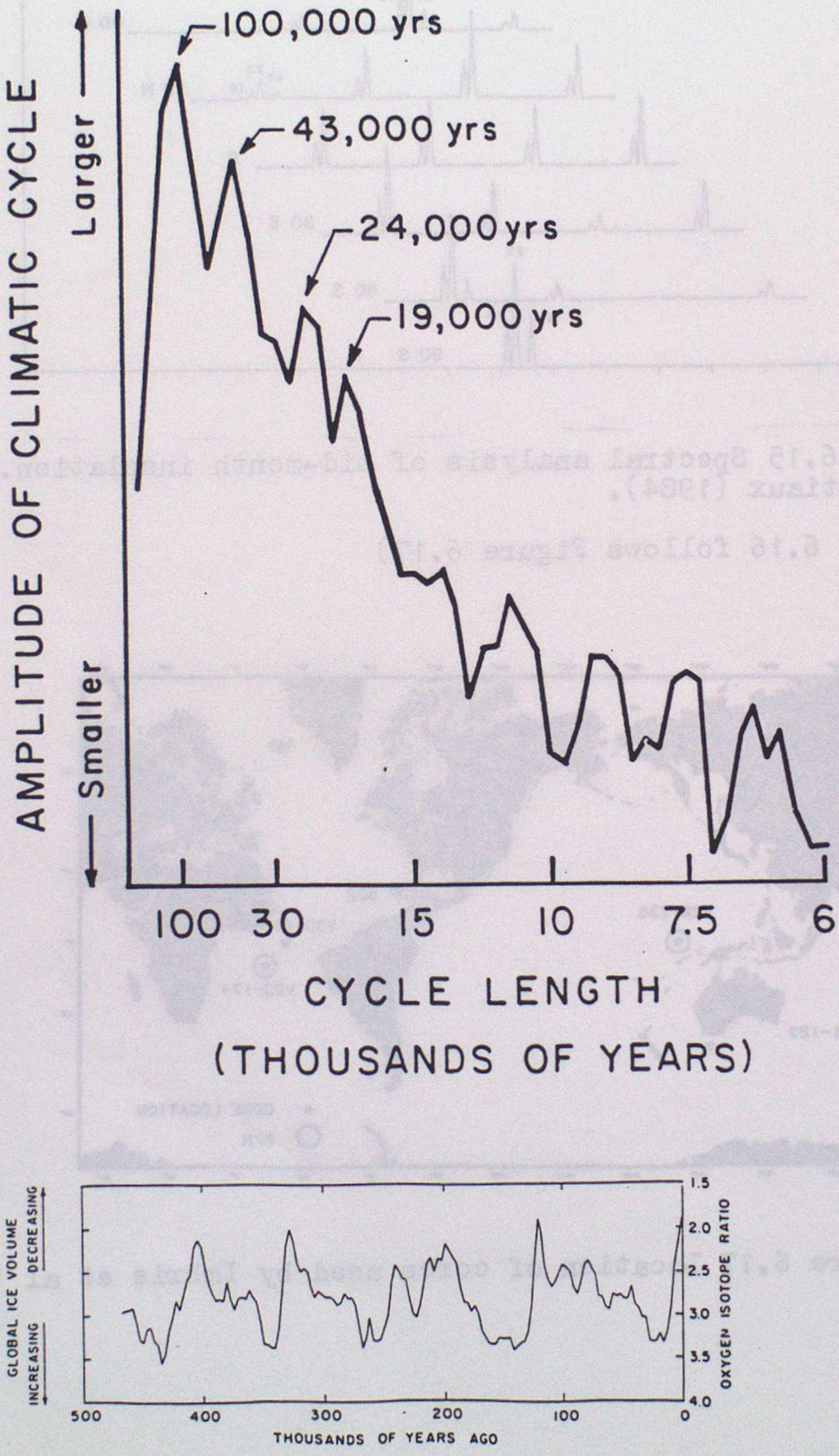

Figure 6.16 Isotopic measurements made on two Indian Ocean cores (below) and the resulting power-spectrum (above). From Imbrie and Imbrie (1979).

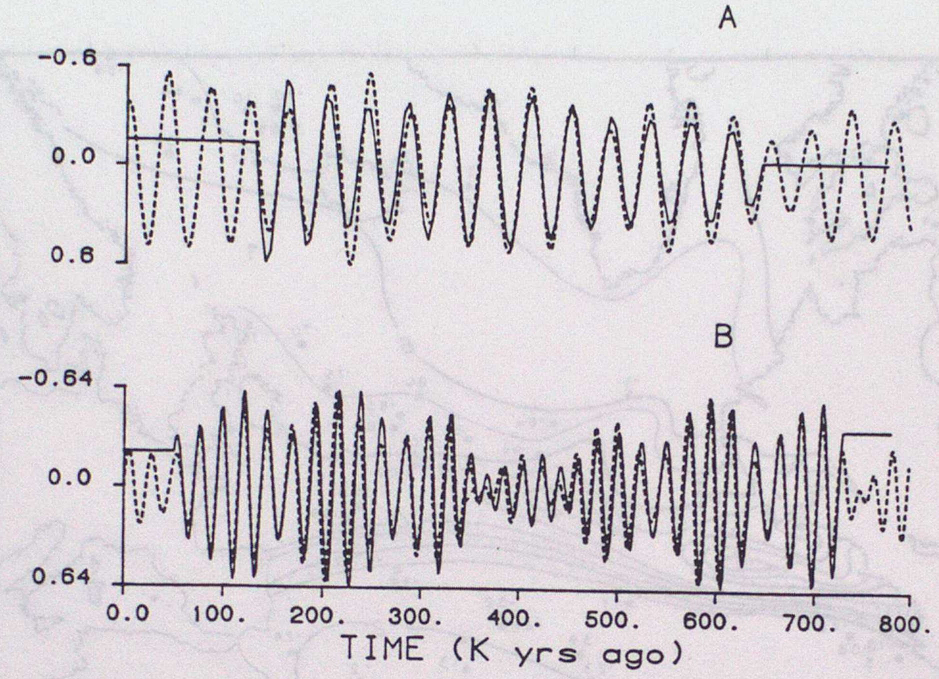

Figure 6.18 Match between oxygen isotope and obliquity(A) and precession (B) curves. Oxygen isotope curves are solid lines obtained by filtering original data. From Imbrie et al (1984)

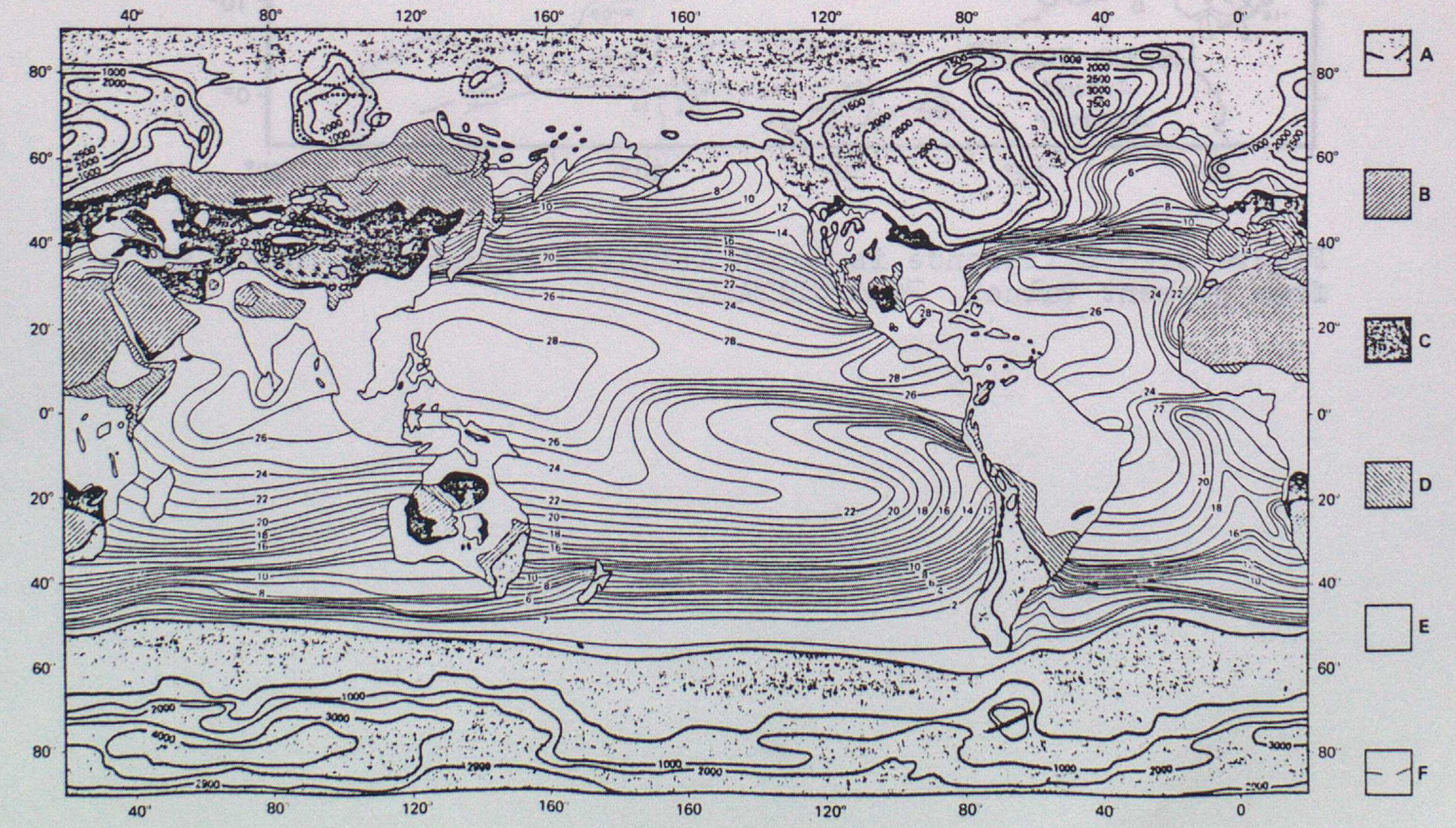

Figure 6.19 Reconstruction of SST and ice extent 18000BP by CLIMAP (August

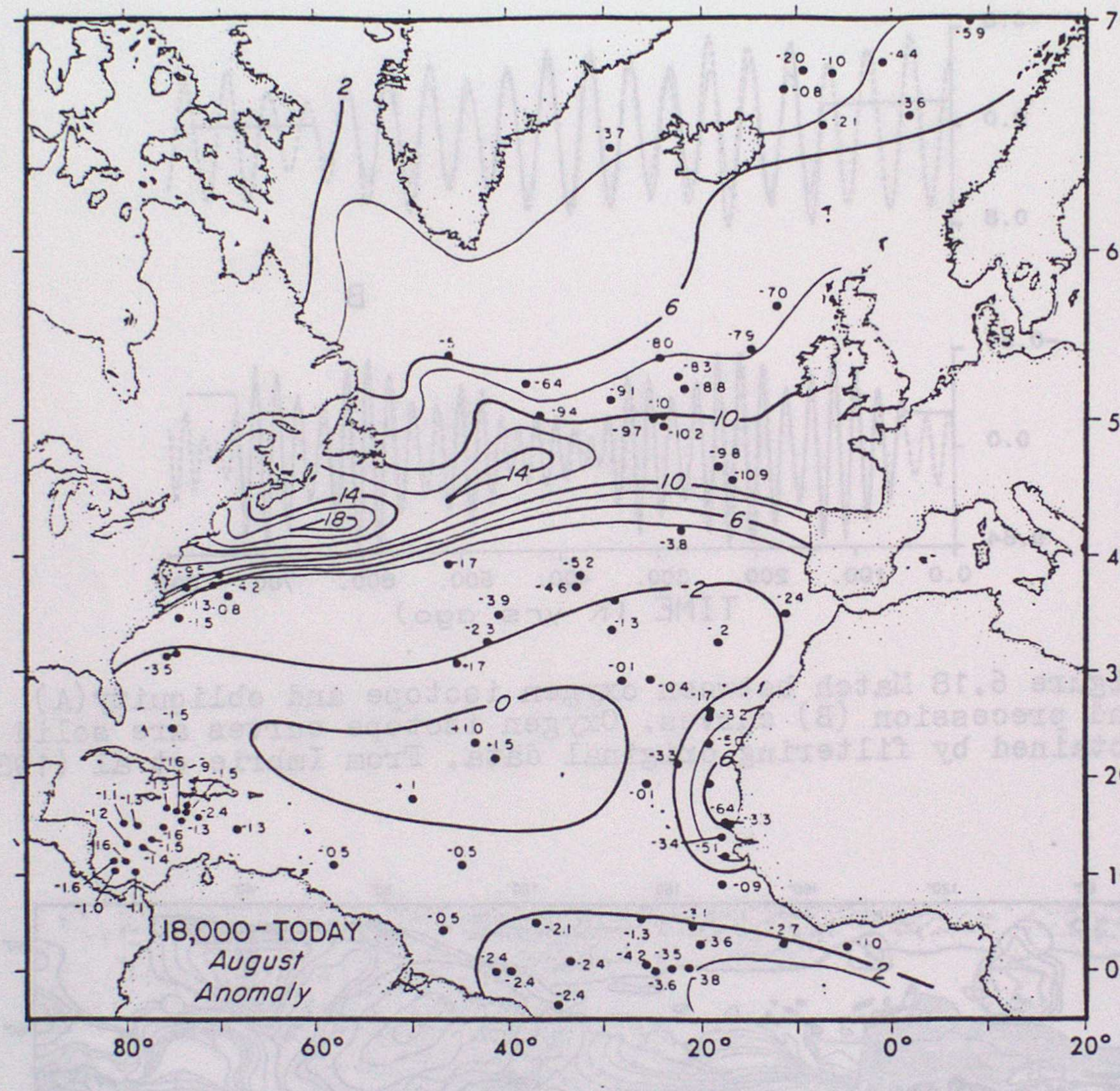

Figure 6.20 Difference is North Atlantic August SST, 18000 BP, from present values. From CLIMAP.

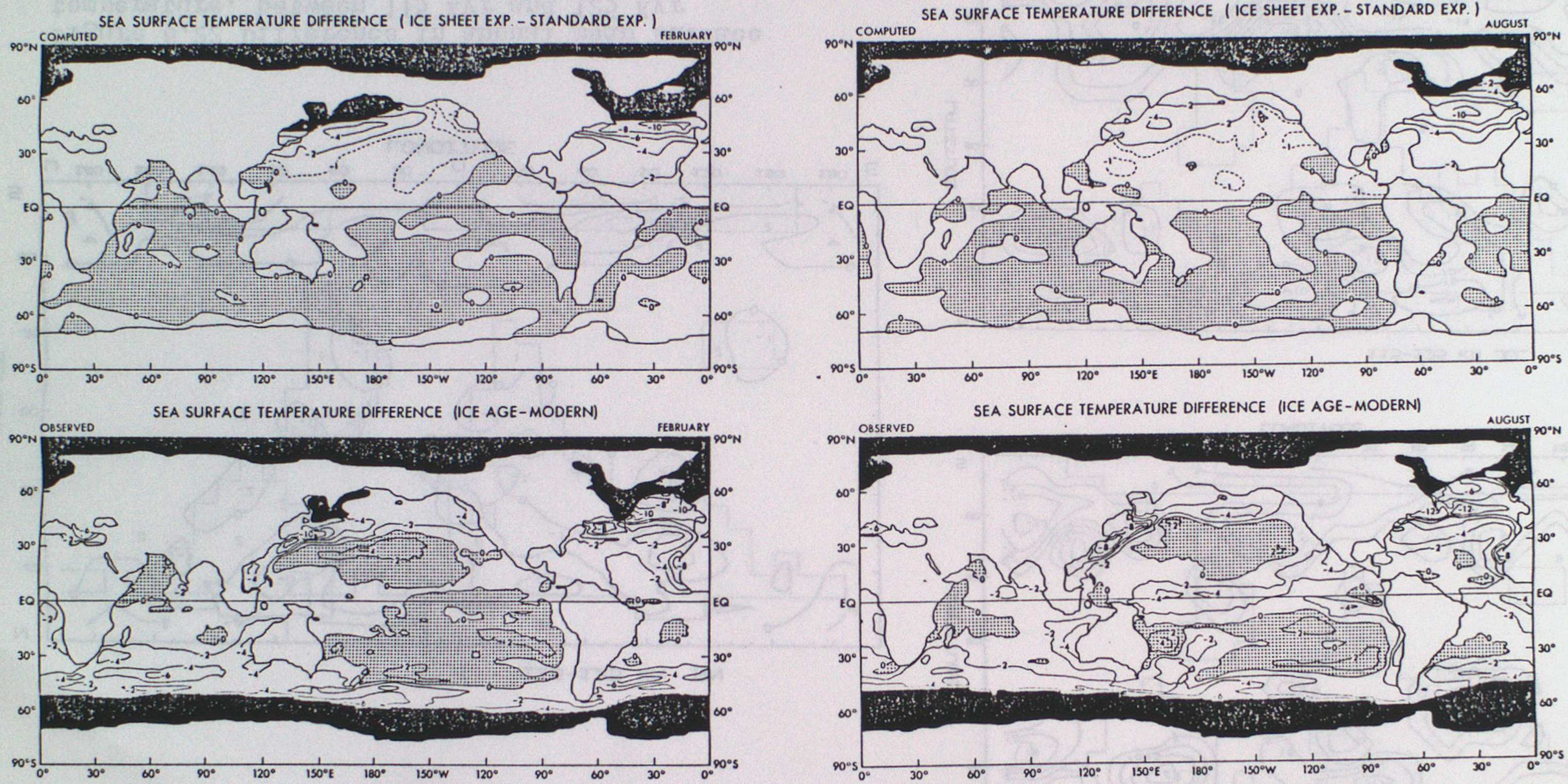

Figure 6.21 From Manabe and Broccoli (1984)

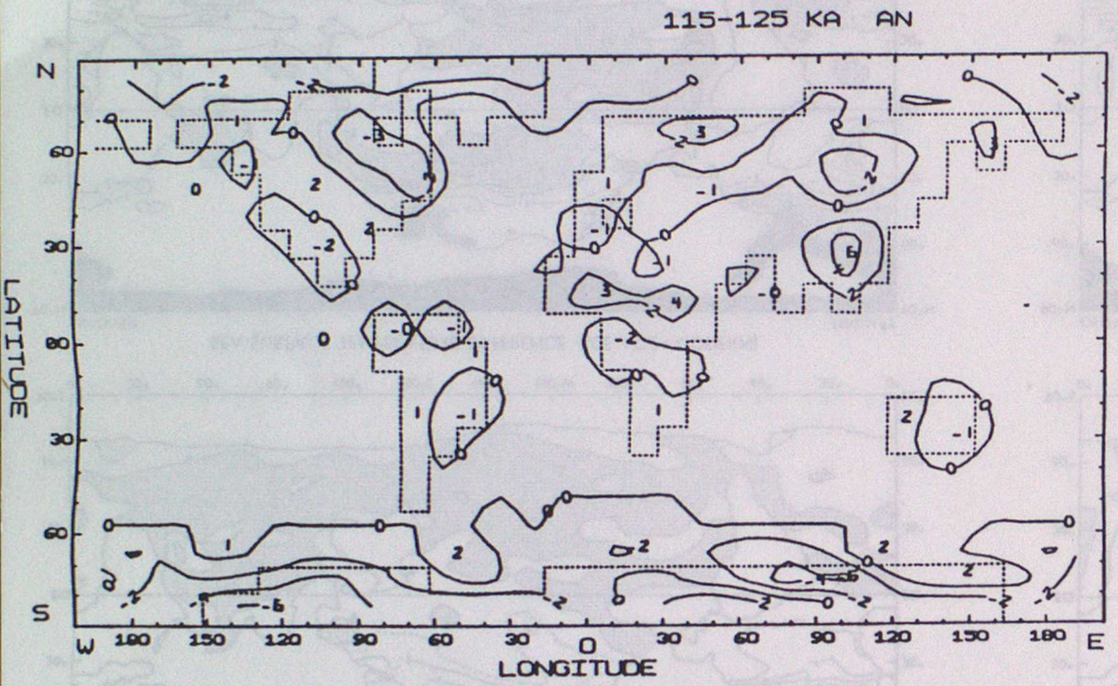

Figure 6.22 Difference in annual mean surface temperature, between 115 Kyr and 125 Kyr simulations. From Royer et al (1984)

Figure 6.23 As Figure 6.22 but for MSL pressure for January (above) and July (below). From Royer et al (1984)

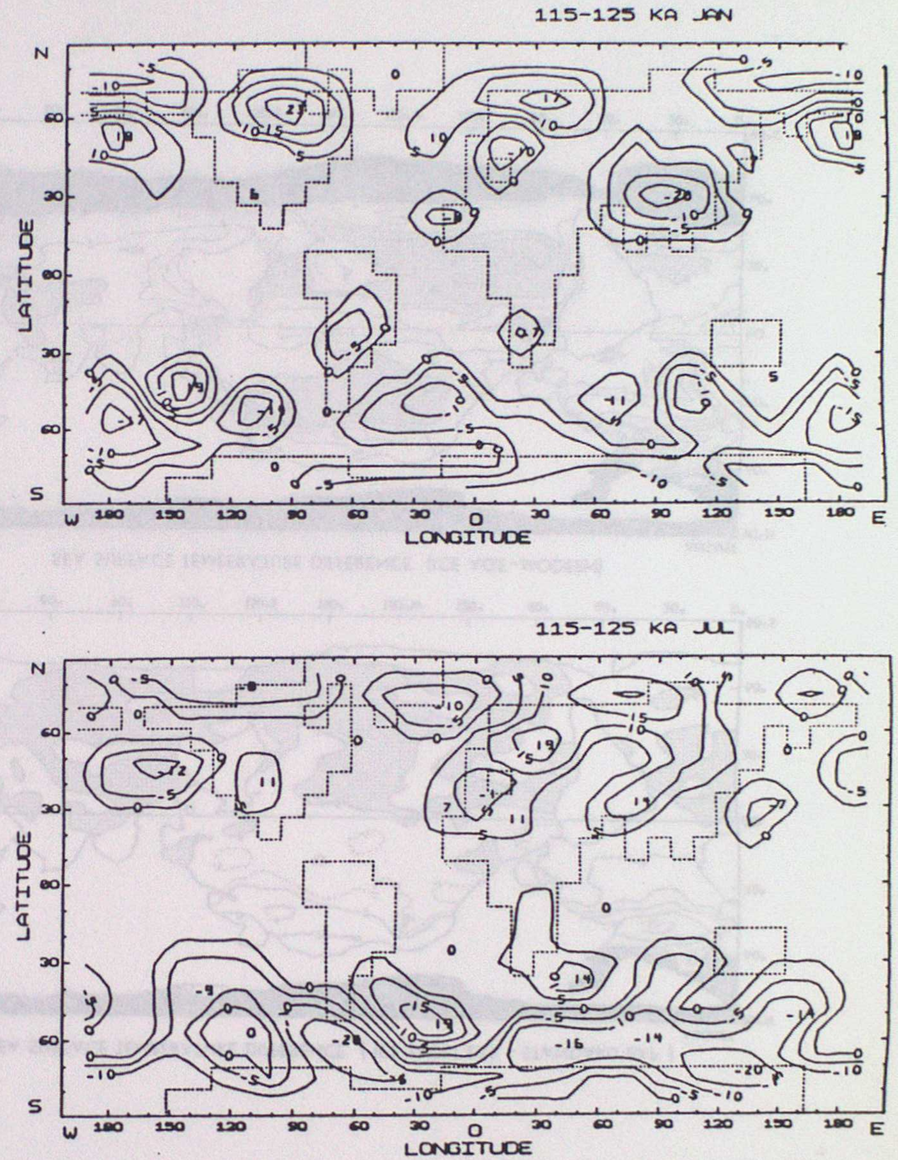

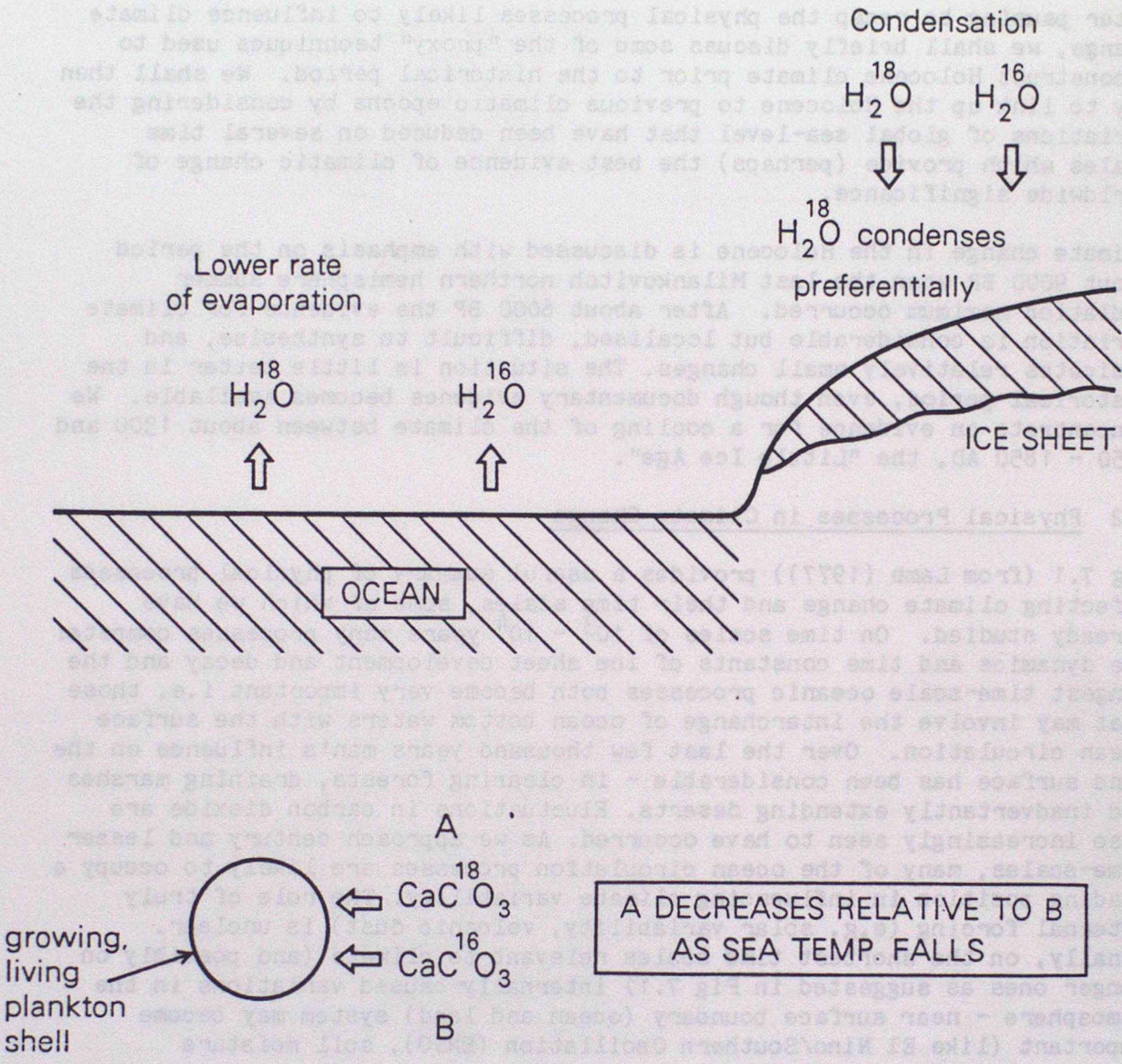

Fig. 6A.1 Oxygen isotope method

DO 3723

ADVANCED LECTURE NO 7

CLIMATES OF THE PAST II - LATE GLACIAL TO LITTLE ICE AGE (c 15000 BP to 200 BP)

7.1 SUMMARY

After pausing to recap the physical processes likely to influence climate change, we shall briefly discuss some of the "proxy" techniques used to reconstruct Holocene climate prior to the historical period. We shall then try to link up the Holocene to previous climatic epochs by considering the variations of global sea-level that have been deduced on several time scales which provide (perhaps) the best evidence of climatic change of worldwide significance.

Climate change in the Holocene is discussed with emphasis on the period about 9000 BP when the last Milankovitch northern hemisphere summer radiation maximum occurred. After about 6000 BP the evidence for climate variation is considerable but localised, difficult to synthesise, and indicates relatively small changes. The situation is little better in the historical period, even though documentary evidence becomes available. We concentrate on evidence for a cooling of the climate between about 1300 and 1650 - 1850 AD, the "Little Ice Age".

7.2 Physical Processes in Climate Change

Fig 7.1 (from Lamb (1977)) provides a useful summary of physical processes affecting climate change and their time scales, some of which we have already studied. On time scales of 10^3 - 10^4 years many processes compete: the dynamics and time constants of ice sheet development and decay and the longest time-scale oceanic processes both become very important i.e. those that may involve the interchange of ocean bottom waters with the surface ocean circulation. Over the last few thousand years man's influence on the land surface has been considerable - in clearing forests, draining marshes and inadvertantly extending deserts. Fluctuations in carbon dioxide are also increasingly seen to have occurred. As we approach century and lesser time-scales, many of the ocean circulation processes are likely to occupy a leading position in influencing climate variability. The role of truly external forcing (e.g. solar variability, volcanic dust) is unclear. Finally, on the shortest time scales relevant to climate (and possibly on longer ones as suggested in Fig 7.1) internally-caused variations in the atmosphere - near surface boundary (ocean and land) system may become important (like El Nino/Southern Oscillation (ENSO), soil moisture variations etc).

7.2.1 Transitivity, intransitivity and almost-intransitivity

A particular problem, raised by Lorenz (1968), is whether the climate is internally stable. Non-linear systems far simpler than the atmosphere - cryosphere - ocean system display a tendency to fluctuate in an irregular manner between two or more internal states (Fig 7.2). In a transitive system, a climate state B will approach a new state A after the climate system has been forced by new boundary conditions appropriate to state A. So given boundary conditions correspond to a given climate. In an intransitive system B stays unchanged despite the new forcing. (e.g. the "white earth" stays white (lecture 6) even when the solar constant increases by reasonable amounts). A third type of behaviour is one where the system stays in state B despite the new forcing but after some time it starts to shift toward A where it might remain - or perhaps spontaneously shift back to B. This "flip-flop" behaviour is called "almost intransitive". Until recently, at least, many climatologists considered that ice-age-interglacial fluctuations were quite likely to have been the result of an almost intransitive process of this kind.

7.3 Methods of Studying Post-Glacial Climates

Lamb (1977) gives an extensive description of methods while Critchfield (1983) and Crane (1981) provide a useful summary. The subject is vast. I shall list and describe a few of the main techniques, but see lecture 6 for some other methods. Fig 7.3 is a diagrammatic summary of some of the techniques.

(1) RADIOMETRIC METHODS FOR DATING

These involve the decay of radioactive isotopes contained in the material being studied; the ratio of the concentration of a radioactive to a non-radioactive isotope of a given element is a measure of the age of a sample. The most usual method for dating Holocene organic material uses the decay of ^{14}C to ^{12}C. ^{14}C is continually created in the atmospheric carbon dioxide by cosmic rays (but not at quite a constant rate due to the variable effects of solar-caused interplanetary magnetic fields). Fig. 7.4 gives an idea of the accuracy of this technique. The technique is not very useful for young samples (less than 150 years old) partly because of the long half-life of ^{14}C (5700 years) and partly because man has changed the proportion of ^{14}C in the atmosphere, and thus in organic samples, through fossil fuel burning; the resulting carbon dioxide contains a higher proportion of ^{12}C than does the naturally occurring carbon dioxide in the atmosphere.

Other methods include (1) the protoactinium-ionium method (the decay of ^{231}P to ^{230}Th, an isotope of thorium known as ionium), whose standard error of dating is about $\pm$ 1000y for ages 7000 BP - 30000 BP: this decay process has been used occasionally to date deep-sea cores. (2) The uranium -thorium method: this includes several radioactive decay techniques one of which involves the decay ^{234}U to ^{230}Th (ionium) with a half life of 75000 years; the method has been used to date fossil coral reefs which provide important evidence of past sea-level fluctuations.

(2) VARVE CHRONOLOGY - DATING AND CLIMATIC EVIDENCE

Varves are annual layers of silt and clay deposited on the bottom of certain lakes and ponds which are subject to freezing in winter and thawing in summer. In winter, ice prevents other than fine sediments from settling to the bottom of the lake; in summer a flux of fresh water brings in coarse sediments. Successive years will exhibit different thicknesses of coarse sediment when a core is taken through the sediments. If the varves are of climatic origin, parallel dating of lake beds in a region is possible through matching of varve thickness, (Fig 7.5). When the lakes are buried under glaciers, no varves are formed so a comparison of varves in different lake beds can indicate when and where glaciers retreated in a region if parallel dating of the varves can be successfully done. Nearly absolute dating is occasionally possible, depending on the effects of more recent climate variations on the varves previously laid down and on a lack of disturbance to the varves by burrowing creatures, floods etc. Fossil lake varves provide powerful evidence for the geography and timing of the retreat of the Scandinavian ice-sheet in the early Holocene period for example.

(3) GROWTH OF LICHENS - LICHENOMETRY

Lichens reaching newly exposed rock-faces after glacier retreat exhibit (after an initial growth flush) remarkably constant growth rates. Measurements of the sizes of the largest lichens present provide evidence of the timing of glacier retreat (for the last few hundred years only).

(4) POLLEN DATING, SOIL CHANGES AND EVIDENCE FOR PAST CLIMATES

Pollen dating is a technique for use on land whose approach parallels the study of changes in the species of foraminifera in lecture 6. By studying the present relationships (ranges and limits) of trees, flowers and shrubs to climate and the density of (very durable) fossil pollen grains left in the soil beneath, it is possible to guess at previous climates by extracting, in widespread locations, cores of soil and identifying and dating the fossil pollen grains. The method is not easy to use as trees may take a long while to migrate after a climate change, disease may strike widely and trees and plants compete in complex ways, even in a constant climate. Nevertheless, with the aid of ^{14}C dating and the study of associated past changes in soil type, such as drying out of peat bogs or their re-establishment, it has been possible to construct detailed pictures of Holocene climate variation in many parts of the world using this technique.

(5) LEVELS OF OLD LAKES

Geological evidence of past lake shorelines can register changes in the balance between local precipitation and evaporation, given that there have been no past tectonic changes, and that the geography of supply and outlet channels has not altered. Dating of the old shorelines can be done using ^{14}C techniques or by studying fossil varves etc.

(6) DENDROCHRONOLOGY - "TREE RINGS"

This technique is based on the observed annual increment of tree growth, the tree ring, and has been mainly used in middle and high latitudes (Fig 7.5). A close relationship between annual rainfall or temperature and growth rings of trees under climatic stress was demonstrated by A E Douglas, an American, early this century. This relationship includes the longest living of all trees, the bristlecone pine of SW USA (oldest specimens 6-8000 years old). Recently the technique has been extended to forest trees like oak living in W. Europe, where tree rings reflect (mainly) May-September climatic conditions, though in a complex way. Dendrochronology is controversial as complex statistical procedures are needed to allow for many non-climatic factors like ageing of the tree, disease, competition, "weather" factors like isolated late frosts, and the fact that the remaining climatic response itself is often complex. The chief reference work is Fritts (1976). Dendrochronology has now been extended to other aspects of tree growth, such as the amount of ^{18}O in a tree ring which can be used, with care, as a paleothermometer.

(7) BEETLES

It is believed by some workers that insects react quickly to climate change; their ancient remains in soils can be very numerous and can be ^{14}C dated. Beetles have apparently shown almost no tendency to evolution over the last 250000 years or so. By studying today's distribution of beetles, past temperatures (mainly summer temperatures) can be inferred from the past distribution of the remains of different beetle species.

(8) RAISED BEACHES AND CORAL REEFS

It is sometimes possible to date raised beaches and, especially, old coral reefs. Corals only grow at or down to about 20-30 m below sea-level. If slow tectonic movements steadily raise reefs, a past, constant sea level is indicated as an extended almost horizontal growth of the exposed fossil reef; rapid falls in sea level will produce rapid downward growth from this level. If the rate of tectonic movement is just correct, a series of stepped surfaces will be created above the changing shore-line. Fig 7.6 shows the most famous example, in New Guinea, which has been used to support the timing of the ice-age-interglacial cycles inferred from deep-sea cores and the Milankovitch radiation cycles.

7.4 Sea-level Variations

Fig 7.7 (A) shows a reconstruction (Lamb (1977), p114) of sea-level variations from the mid Tertiary (20 m.y) to the present. The glacial-interglacial cycles are indicated (some are omitted). A long-term fall in sea level seems to be superimposed on the glacial-interglacial cycles; Lamb suggests that this fall may be due to crustal sinking under the ocean floor. The rise at the end of the curve of about 100 m is consistent with the total volume of ice that is believed to have melted since 18000 BP. Fig 7.7 (B) shows a more detailed reconstruction of sea-level over the last 200000 years while Fig 7.7 (C) gives details of changes in Holocene sea-level, from diverse indicators, due to Fairbridge (1978).

Holocene sea-level reached a global maximum (corrected for tectonic movements) about 4000 BP and has declined by about 4 m since then. There are suggestions of mid-Holocene fluctuations to levels at or below the present level. Fairbridge claims that the sea-level fluctuation about 4900 BP (during the regions of the early Pharoahs of Egypt) was abrupt, with a 5 m increase in perhaps 250 years. If true, this corresponds to a melting of more ice than currently exists on all mountain glaciers together (excluding the Greenland and Antarctic ice caps).

7.5 Post-Glacial Climate Fluctuations and the Melting of the Laurentide (N. American) and Scandinavian Ice Sheets

7.5.1 General Scheme of temperature Fluctuations

The details of the Holocene warming are best known in the N. Hemisphere and there is no guarantee, for example, of a global synchroneity in temperature change. Fig 7.8 (A) shows an interpretation of the evidence for the timing of temperature changes in Central England (Lamb (1977), p232). The warming was not, apparently, continuous but interrupted by at least one major cooling c. 10000-11000 BP (others have been suggested). The prior, warm, stage at about 12000-11000 BP is known as the Allerod and the cold period afterwards (about 10800-10200 BP) is called the Younger Dryas. In the Allerod summers of Central England, fossil beetle evidence suggests a mean temperature of 18°C or so i.e.probably warmer than now.

Going far afield, there is only a little evidence of the Allerod/Younger Dryas oscillation from the New Guinea mountains (Fig 7.8 (B)) (in Fig 7.8(B) Sirunki is below the ice age glaciation level and the evidence comes from pollen) though warming occurred up to 11600 BP and after 11600 BP a small glacial advance occurred on Mt Carstenz (5000m), West Irian, Indonesia (where glacier snouts currently reach down to 4300 m). However Fig 7.8 (B) taken from Bowler et al (1976), is striking in that it indicates a large warming from 18000 BP - 5000 BP when the CLIMAP SST reconstruction (lecture 6) suggests that SST in the tropical W Pacific region at 18000 BP was only about 1.5-2.0°C below todays values. Equally, large, roughly contemporary, high mountain warmings have also been inferred by several workers in the equatorial Andes. However an increase of 2°C in SST could give rise to nearly double that increase at 4000 m near the equator as equivalent potential temperature, rather than air temperature, should have changed nearly uniformly with height i.e. the lapse rate probably changed (a modern example is given in lecture 5, Pt I of the fluctuations of tropical troposphere temperatures and lapse rate associated with El Nino- Southern Oscillation described by Pan and Oort (1983)). There is support for the Allerod-Younger Dryas temperature oscillation in two Greenland Ice cores (Dansgaard et al (1982)), at Dye 3 and Camp Century; (see Fig 7.9 (A), especially the area of the Figure between "3" and "2").

A fluctuation from wet (Allerod) to dry (Younger Dryas) conditions in the Colombian Cordillera (5°N, 2850 m) is reported in Flohn (1978); a hint of a decrease of temperature and a strong indication of a decrease of CO_2 (by about 100 ppm) is reported for the same period from the Antarctic "Dome C" ice core (Delmas et al (1980)) (Fig 7.9 (B)). This core also shows a rise in CO_2 (trapped in the ice) from 15000 BP -13000 BP (dates uncertain by say $\pm$1000) of about 100 ppm, (from 190 ppm to 300 ppm) suggesting that the waxing and waning of world-wide temperature was accompanied by quite large changes in CO_2 on more than one time scale. Fig 7.10 shows a reconstruction of mid-latitude tree lines, 13000 BP to now. Fig 7.11 summarises the present, rather vaguely understood, picture of the broad changes in mid-latitude N. Hemisphere temperatures on several time scales over the last million years (Lamb (1977), p334) including the Holocene (10000 year) time scale.

7.5.2 The recession of N. Hemisphere ice sheets in the early Holocene

This description is mostly taken from Lamb (1977). Figs 7.12 (A) - (C) show reconstructed positions of the ice sheets for (a) 18000 BP, (b) the Allerod warm phase and (c) the Younger Dryas. Ice had nearly disappeared from Scotland by the end of the Allerod but then strongly readvanced in the Scottish Highlands for a few hundred years in the Younger Dryas (known as the Loch Lomond Readvance), an advance that has left many traces in old moraines etc and which occurred near the N. Hemisphere Milankovitch radiation maximum. Fig 7.13 shows a reconstruction of the stages in the contraction of the Scandinavian Ice Sheet; the associated emergence of the Baltic is shown in Fig 7.14 (A) - (D) (a lot of the evidence comes from old shore lines). At first the Baltic was probably a fresh water lake (Fig 7.14 (A)), then as sea-level rose it became the salt "Yaldia Sea", connected now with the Atlantic. The land continued to rise ("isostatic uplift") as the burden of ice disappeared and the Baltic became fresh again (8000 BP). As sea-level rose further, due to melting of the Laurentide ice sheet in N America, the Baltic became salt again. At present the land is rising by up to 1 cm a year in the northern Gulf of Bothnia (near 65°N) so widespread re-emergence of land may occur there in the next 1-2 thousand years unless global sea-level rises. Fig 7.15 shows an old, but apparently acceptable reconstruction of the geography of Britain and NW Europe 1000-2000 years before sea-level rose high enough to turn Britain into an island. Fig 7.16 shows isochrones of the withdrawal of the Laurentide ice sheet. Slowing of the retreat in the Younger Dryas period is suggested. Extensive remnants still exist on Baffin Island (eg Barnes Ice Cap), Devon Island and Ellesmere Island.

7.6 The Holocene Milankovitch Radiation Maximum - the Sahara and the Sahel

There is considerable evidence of increased rainfall in the southern Sahara and the Sahel about 4000-9000 years ago. Cave and rock paintings of many species of savannah animals (being hunted or farmed) are found from the latter part of this time (an excellent example is shown in Lockwood (1979), p.121). Widespread evidence of expanded lakes occurs in the region (Nicholson and Flohn (1980)), including an enormously extended Lake Chad (Lake Megachad), and other equatorial African and Sahel lakes were larger too (Fig 7.17). Kutzbach and Guetter (KG) (1984) have carried out two AGCM experiments for radiation conditions for 9000 BP to determine if a high resolution model (the NCAR Community Climate model) indicates that a more vigorous African and Asian Summer monsoon was likely during the Holocene radiation maximum. KG carried out two types of anomaly-control experiments:-

(a) Perpetual January and July experiments with 9000 BP radiation and an extensive Laurentide ice sheet in the anomaly experiments; present day radiation and ice in the control experiment.

(b) Similar, but no Laurentide ice sheets at 9000 BP.

Climatological-mean SST is believed to have been similar, averaged over the year, but with a slightly larger annual range (perhaps 1°C); the model was given modern climatological mean SST in all experiments however. Each experiment was run for 120 days and the final 90 days averaged. The main results - global maps of the differences between anomaly and control experiments - are shown in Fig 7.18 (A) - (C) (surface temperature) and 7.19 (A) -(C) PMSL.

In winter, N.Hemisphere land at higher latitudes is simulated to be colder at 9000 BP than now as a result of the reduced winter radiation but in summer the land is much warmer than now as radiation is larger i.e. the seasonal range increases (by 3°C over N. Hemisphere land as a whole). In summer, the presence of the Laurentide ice sheet only affects temperatures just downstream of its position (over the N. Atlantic); just upstream, (Fig 7.18 (B)) its presence does not change the surface temperature, which is considerably warmer than now in summer. In winter the Laurentide ice sheet reduces PMSL considerably over the N. Atlantic/W. European region by inducing a large lee trough. In summer, the 9000 BP monsoon circulation over N. Africa and S. Asia is considerably enhanced (Fig 7.19 (B)). Precipitation increases in the area from 30°E - east Asian coast and south of 40°N by 20% according to KG. Fig 7.20 summarises zonally-averaged precipitation changes. In July increased precipitation associated with the ITCZ at 9000 BP is shown; the vertical bars represent 1 standard deviation of the control integrations (1050 model days were available for modern (control) conditions). So given the archaeological evidence as well it is very likely that summer rainfall was larger in the Sahel/Sahara at 9000 BP than now and probably for some thousands of years afterwards.

7.7 Holocene maximum (hypsithermal)

Figs 7.10, 7.11 suggested that rather modest changes of worldwide climate have occurred since 5000 BP (3000 BC), at least up to 1000 AD. Details are difficult to unravel but about 3000-3500 BC there is evidence of a short period cooling (Piora Oscillation) in the N. Hemisphere. The details of Holocene climate are currently being pieced together for the whole globe by COHMAP, (Cooperative Holocene Mapping Project) in USA. Many proxy techniques are being used including pollen analysis and deep-sea core analysis. It is hoped to reconstruct a mean picture of climate about every 3000 years since 18000 BP. Fig 7.21 is an example of vegetation mapping in N. America for 10000 BP, 6000 BP and 1500 AD (Kerr (1984)). Note the close approach of forest to the margin of the Laurentide Ice Sheet at 10000 BP.

About 4000 BP (2000 BC), the advanced Harrapan culture of the now Thar Desert in Rajastan (N India) declined and disappeared. Fig 7.22, from Lamb (1982), suggests this was due to a strong reduction of summer monsoon rainfall towards current conditions. The climatic evidence has mostly been obtained from pollen cores drilled beneath the beds of former lakes that now occupy positions between sand dunes.

Subsequently there is evidence that about 500 BC a sharp cooling occurred (the so-called sub-Atlantic pessimum) when temperature may have declined widely by about 2°C and the mountain glaciers advanced. In classical Roman times the climate was probably rather like nowadays but in early Rome climate was probably cooler according to the testimony of several Latin authors. About 800 AD, possibly later, there is evidence of a climatic warming in the middle and high N. Hemisphere latitudes. This was the time (870-950) of the settlement by the Norse of, first, Iceland and then, Greenland. In the High Middle Ages vineyards were common in England and good quality wines were produced where wine growing is hazardous nowadays. This was the so-called Little Optimum (at least in W. Europe) and shows well on the graph of temperatures of the last 1000 years (Fig 7.11). However it is not clear whether the Little Optimum represents a regional or a more widespread change in climate. Growth of some of the Bristlecone pines in south-west USA when near the tree line is believed to be controlled by summer temperature. Fig 7.23A (from two locations in California) shows slight evidence of the Piora temperature oscillation, the 1000 BC - 500 BC cool period and the cooling since the Medieval Optimum; the latter does not show as a peak but rather as a halt in a steady decline of temperature. The Alpine tree-line curve (Fig 7.23B) is broadly similar in shape except it shows a more definite medieval climatic optimum, and it does not extend back to the Piora oscillation.

7.8 Little Ice Age

As will be shown in lecture 8, it is not necessarily true that if one hemisphere cools or warms that the other responds similarly. Furthermore, changes in the structure of the mid-latitude long waves can give an impression of global warmth or coldness if sampling is longitudinally restricted. Having said this, the evidence for a "Little Ice Age" is quite good, but not all areas were necessarily colder than now as superimposed changes in circulation patterns would probably have occurred. Fig 7.24 from Lamb (1977) shows the results of a survey of historical documents and weather records in Europe and Japan that attempts to summarise the changing frequency of cold winters in these two areas 120° of longitude apart. The diagram suggests that Japanese winter temperatures have fluctuated largely out of phase with those of European winters. However there is geographically widespread evidence for a cooler climate, worldwide, from after 1400 AD until about 1850. Fig 7.25, also from Lamb (1977), shows evidence of century time-scale temperature variations from New Zealand, (accuracy of reconstruction unclear) while the Greenland Ice cores also support a cooler climate (the dating should be excellent), though Dome C only gives slight support. It is possible to use ^{18}O measurements in the wood of oaks to determine past changes of temperature, at least in a relative sense. Dating is done by counting tree rings and the ^{18}O concentration is measured in the individual rings. Fig 7.26, from Lamb (1977), shows such a reconstruction for some trees in Germany. Freezing of rivers and canals also became more frequent in Europe around 1600-1800. Most impressive are the results of widespread investigations of the moraines left by mountain glaciers (Fig 7.27 gives examples). In many parts of the world there is increasingly strong evidence that the glaciers on many mountains were the most advanced around 1600-1800 AD since the time of the Younger Dryas. (LeRoy Ladurie (1971) gives an excellent description for the Alps).

There is no doubt that conditions in the Iceland-Greenland area became much colder after 1200 AD and especially after 1550 AD. In lecture 3 we showed a diagram of the reconstructed variation of sea-ice around Iceland in weeks/year; the period around 1800 seems to have been the worst for sea-ice. The Norse colony in S. Greenland established around 900 AD probably died out in the fifteenth century as climatic conditions became worse, sea ice prevented access (from Iceland and Europe) and crops failed (LeRoy Ladurie (1971)). Fig 7.28 shows the variation of ^{18}O in a Greenland ice core (Dansgaard et al (1975)); absolute dates are probably not accurate but a tendency to cooling after about 1100-1200 AD is clearly shown as is the rise in temperature at the beginning of the twentieth century. Remember that temperature increases to the right on these diagrams. Lamb also describes documentary evidence of observations of extensive sea ice flows around the Faeroe Islands in a few winters in the seventeenth century and once or twice, ice floes reached the Shetland Isles. Eighteenth century travellers frequently mention permanent snowbeds in the Cairngorms. In recent years lichenometry has been used to indicate that certain hollows in the Scottish mountains might well have been permanently filled with snow for lengthy periods up to the middle of the last century.

Despite this evidence, more research is required to show whether the period 1600-1800 was cold worldwide. However the latter part of the Little Ice Age overlaps with the instrumental period so we can pursue this problem a little more in the next lecture.

REFERENCES TO ADVANCED LECTURE 7

AHLMANN, H.W. (1953) Glacier Variations and Climatic Fluctuations. Bowman Memorial Lecture. New York (American Geog. Soc.).

BOWLER, J M; HOPE, G S; JENNINGS, J N; SINGH, G; and WALKER, D (1976) Late Quaternary Climates of Australia and New Guinea. Quaternary Res., 6, pp 359-394.

BRYSON, R.A., WENDLAND, W.A., IVES, J.D., and ANDREWS, J.T. (1969) Radiocarbon isochrones on the disintegration of the Laurentide ice sheet. Arctic and Alpine Res., 1, pp 1-14. Boulder, Colorado.

BURROWS, C.J. (1973) Studies on some glacial moraines in New Zealand. II. The ages of moraines of the Mueller, Hooker and Tasman glaciers. New Zealand J. Geol. Geoph., 16, pp 831-856.

BURROWS, C.J. (1975) Late Pleistocene and Holocene moraines of the Cameron valley, Arrowsmith Range, Canterbury, New Zealand. Arctic and Alpine Research, 7, pp. 125-140.

BUTZER, K.W., ISAAC, G.L., RICHARDSON, J.L. and WASHBOURN-KAMAU, C. (1972) Radiocarbon dating of East African lake levels. Science, 175, pp 1069-1076.

CRANE, A J (1981) Techniques for reconstructing Past Climates. In 'Climatic Variations and Variability: Facts and Theories'. Ed:- A Berger. Reidel.

CRITCHFIELD, H J (1983) General Climatology. 4th Edition. Prentice-Hall.

DANSGAARD, W; CLAUSEN, H B; GUNDESTRUP, N; HAMMER, C U; JOHNSEN, S F; KRISTINSDOTTIR, P M; REEH, N (1982) A new Greenland Deep Ice Core. Science, 218, pp 1273-1277.

DANSGAARD, W., JOHNSEN, S.J., CLAUSEN, H.B. and LANGWAY, C.C. Jr. (1971) Climatic record revealed by the Camp Century ice core. In "The Late Cenozoic Glacial Ages", ed. K.K. Turekian. Yale Univ. Press, New Haven, pp 37-56.

DANSGAARD, W; JOHNSEN, S J; REEH, N; GUNDESTRUP, N; CLAUSEN, H B; AND HAMMER C U (1975) Climatic changes, Norsemen, and modern man. Nature, 255, pp 24-28.

DE GEER, E.H. (1954) Skandinaviens geokronologi. Geol. Foren. Forhandl., (GFF), 76, pp. 299-329. Stockholm.

DELMAS, R J; ASCENCIO J M; AND LEGRAND M. (1980) Polar ice evidence that atmospheric CO_2 20000 yr BP was 59% of present. Nature, 284, pp 155-157.

DENTON, G.H. and KARLEN, W. (1973) Holocene climatic changes, their pattern and possible cause. Quaternary Research, 3, pp 155-205.

FAIRBRIDGE, R.W. (1961). Eustatic changes in sea level. In "Physics and Chemistry of the Earth", Vol. 4, Pergamon Press, London, pp. 99-185.

FAIRBRIDGE, R.W. (1962) World sea level and climatic changes. Quaternaria, 6, pp. 111-134.

FAIRBRIDGE, R.W. (1976) Shellfish-eating preceramic Indians in Coastal Brazil. Science, 191, pp. 353-359.

FAIRBRIDGE, R W (1978) Models of Climatic Change: Global Cycles and Climate. In 'Climatic Change and Variability - a Southern Perspective' Eds: A Pittock et al. Cambridge Univ. Press, pp. 200-211.

FLOHN H (1978) The long-term climatic record: Abrupt events in climatic history. In: 'Climate Change and Variability - a Southern Perspective'. Ed: A Pittock et al, Cambridge University Press, pp. 124-134.

FRITTS, H C (1976) Tree rings and climate. Academic Press.

GEYH, M.A. and JAKEL, D. (1974) Late Glacial and Holocene climatic history of the Sahara Desert derived from a statistical assay of carbon-14 dates. Palaeogeography, Palaeoclimatology and Palaeoecology, 15, pp. 205-208.

GODWIN, H. (1956) The History of the British Flora. Cambridge Univ. Press. 384 pp.

HULTEN, E. (1971) Atlas over vaxternas utbredning i norden. Stockholm (Generalstabens Litografiska Anstalt). 531 pp.

IMBRIE, J. and IMBRIE, K.P. (1979) Ice Ages - solving the Mystery. MacMillan, London.

KERR, R A (1984) "Climate since the ice began to melt", Science, 226, pp 326-327.

KUTZBACH, J E AND GUETTER, P J (1984) The sensitivity of monsoon climates to orbital parameter changes for 9000 years BP: Experiments with the NCAR general circulation model. Milankovitch and Climate, Vol 2, pp 801-820.

LAMARCHE, V.C. (1974) Palaeoclimatic inferences from long tree-ring records. Science, 183, pp 1043-1048.

LAMB, H.H. (1969) Climatic fluctuations. Pp. 173-249 in "World Survey of Climatology" (general Ed. H.E. Landsberg), Vol. 2: General Climatology (Ed. H. Flohn). Elsevier, Amsterdam.

LAMB, H H (1977) Climate: Present, Past and Future Vol 2. Methuen.

LAMB, H H (1982) Climate, history and the modern world. Methuen.

LE ROY LADURIE, E (1971) Times of Feast, Times of Famine: A History of Climate since the year 1000. Trans. B Bray; Doubleday.

LOCKWOOD, J G (1979) Causes of Climate. Edward Arnold, London.

LORENZ, E N (1968) Climatic Determinism. In 'Causes of Climatic Change' Ed: J M Mitchell, Met Monograph 8, pp 1-3. Boston: Amer. Met. Soc.

MARKGRAF, V. (1974) Palaeoclimatic evidence derived from timberline fluctuations. Pp. 67-83 in "Les Methodes quantitatives d'etude des variations du climat au cours du Pleistocene" (Ed. J. Labeyrie). Colloques internat. du. C.N.R.S. No. 219, Paris (C.N.R.S). 317 pp.

MITCHELL, J.M. (1963) On the world-wide pattern of secular temperature change. Pp 161-181 in "Changes of Climate": Proc. UNESCO/WMO Rome 1961 Symp. (UNESCO Arid Zone Research Series, XX). Paris.

MORNER, N.A. (1969). The late Quaternary history of the Kattegatt Sea and the Swedish west coast. Sveriges Geologiska Undersokning, Ser. C, No. 640, 487 pp.

NATIONAL ACADEMY OF SCIENCES (1975). Understanding Climatic Change - A Program for Action. Washington, D.C.

NICHOLSON, S E AND FLOHN, H (1980) African environmental and climatic changes and the general atmospheric circulation in Late Pleistocene and Holocene. Climatic Change, 2, pp 313-348.

PAN, Y.H. and OORT, A.H. (1983) Global climate varaitions connected with sea surface temperature anomalies in the eastern equatorial Pacific for the 1958-73 period. Mon. Weath. Rev., 111, pp. 1244-1258.

TEN BRINK, N.W. and WEIDICK, A. (1974) Greenland ice sheet history since the last glaciation. Quaternary Research, 4, pp. 429-440.

VEEH, H.H. and CHAPPELL, J. (1970) Astronomical theory of climatic change: support from New Guinea. Science, 167, pp 862-865.

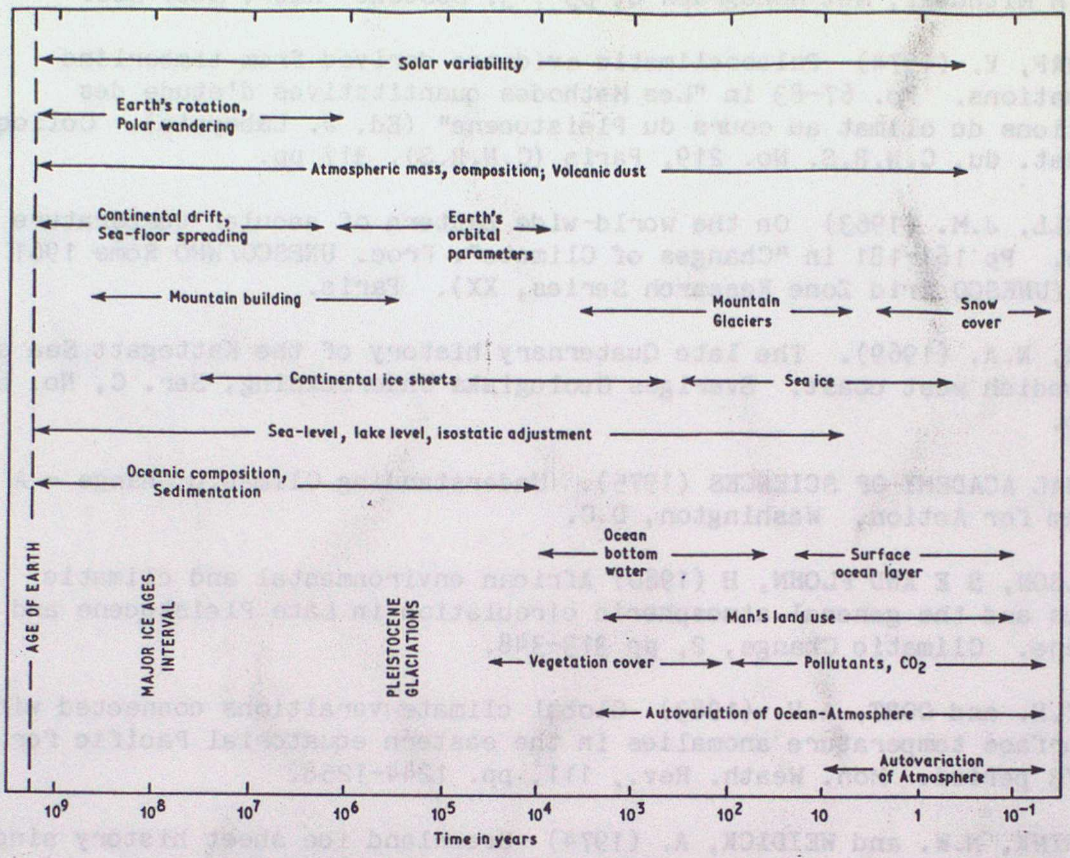

Summary diagram to show the characteristic time-scales over which changes in various influences upon the global climate operate.
(*Adapted from a diagram by* W. L. GATES.) Figure 7.1 From Lamb (1977)

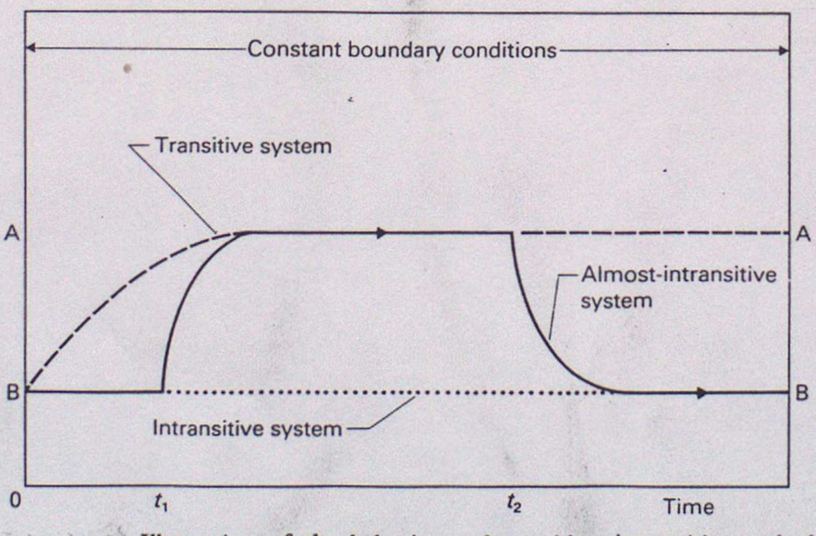

Illustration of the behaviour of transitive, intransitive and almost-intransitive climatic systems with respect to an initial climatic state B. The climatic state A is an alternative bistable state under the same boundary conditions (*after US National Academy of Sciences, 1975*).

Figure 7.2

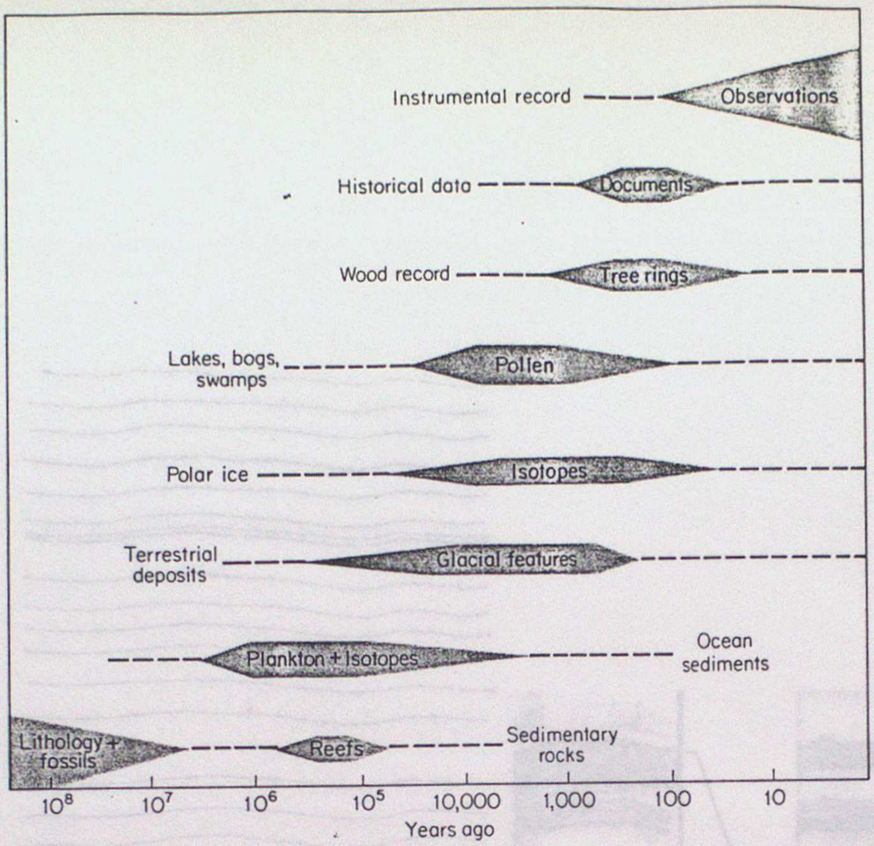

Types of evidence for climatic change and their approximate time scales. (After Bernabo, *EDIS*.)

Figure 7.3 From Critchfield (1983)

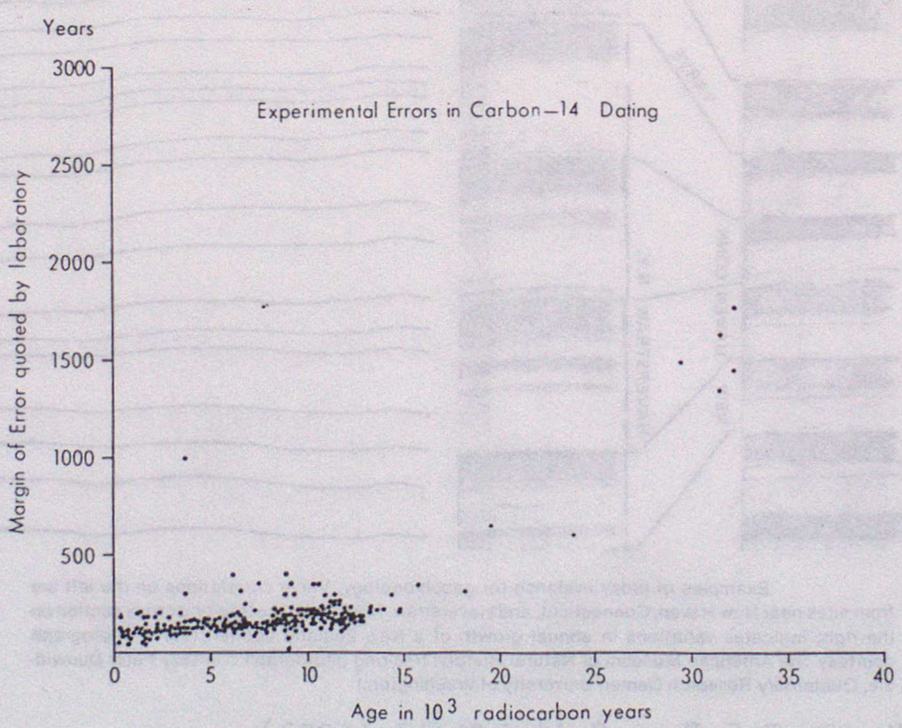

Experimental errors (i.e. random error) in radiocarbon dating. The plotted points are estimates of one sigma error published with the age results of measurements made in the Cambridge, Copenhagen and Washington University radiocarbon laboratories between 1959 and 1968. (*From Radiocarbon, vols. 1–10.*)

Figure 7.4 From Lamb (1977)

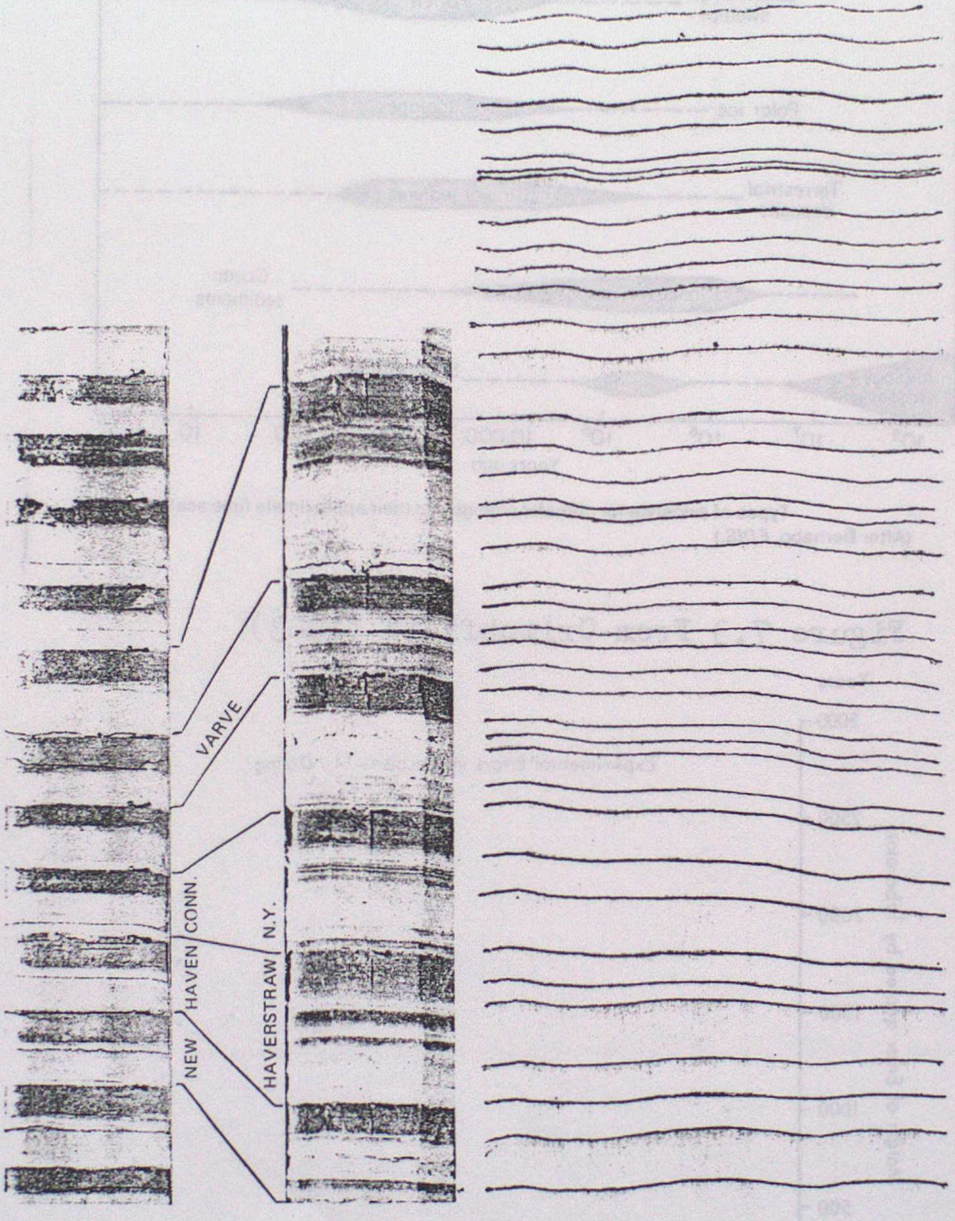

Examples of proxy evidence for geochronology. Varve correlations on the left are from sites near New Haven, Connecticut, and Haverstraw, New York. The tree-ring cross section on the right indicates variations in annual growth of a New Zealand conifer. (Varve photograph courtesy The American Museum of Natural History; tree-ring photograph courtesy Peter Dunwiddie, Quaternary Research Center, University of Washington.)

Figure 7.5 From Critchfield (1983)

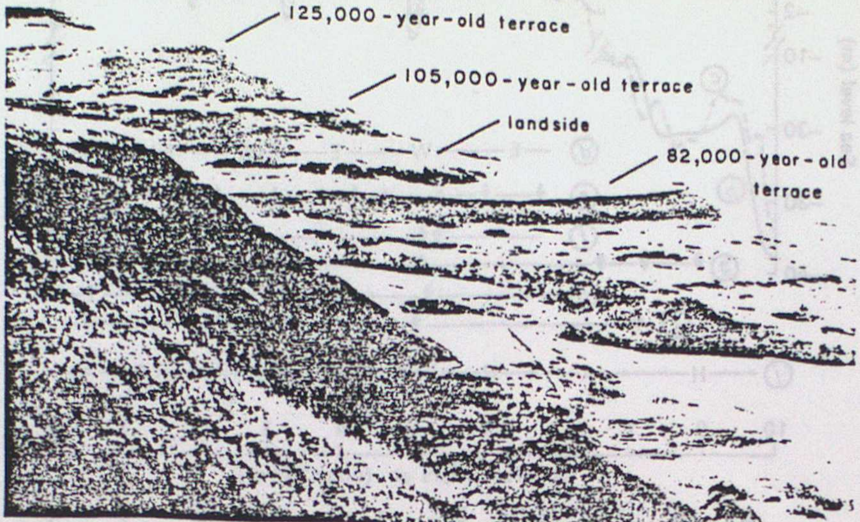

.. Reef terraces on New Guinea. A view along the north coast of the Huon Peninsula, showing uplifted terraces formed by Pleistocene coral reefs. Terraces similar to these were first dated on the Caribbean island of Barbados. (Courtesy of A. Bloom.)

Figure 7.6 From Imbrie and Imbrie (1979)

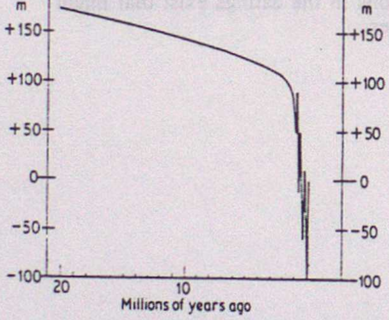

World sea level changes since the late Tertiary (Miocene).

(Ice-age-interglacial variations only schematically indicated – in reduced numbers).

Figure 7.7A From Lamb (1977)

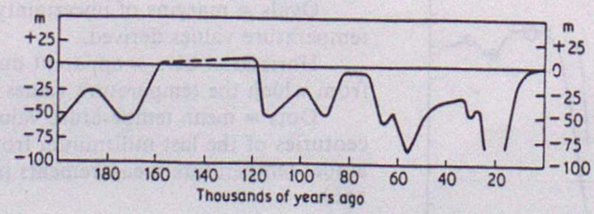

History of world sea level over the last 200 000 years, according to VEEH and CHAPPELL (1970).

Figure 7.7B From Lamb (1977)

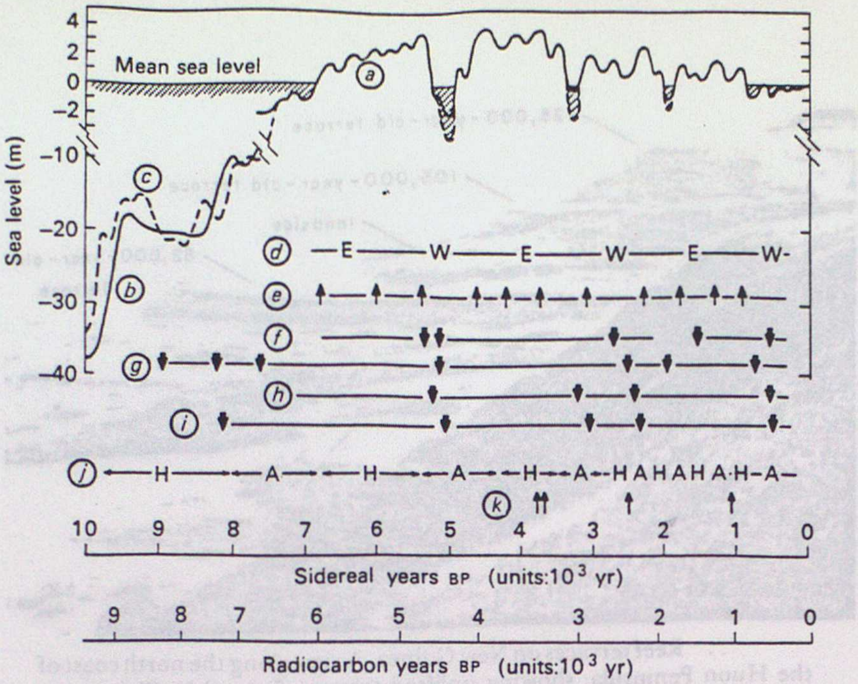

Figure 7.7C
From Fairbrid
(1973)

Trace of eustatic sea level over the last 10,000 years, as indicated (*a*) by an example from Brazil (Fairbridge, 1976), based on radiocarbon-dated beach deposits, coral reefs and Indian middens, for the last 7,000 years, and for the previous 3,000 years by data (*b*) from Scandinavia (Mörner, 1969), and (*c*) elsewhere (Fairbridge, 1961). Note that time is given in both sidereal and radiocarbon years. Comparisons are presented (from top to bottom) with (*d*) the magnetic declination cycle (approximately 2,850 years) with its E–W inflections; (*e*) the $^{18}O/^{16}O$ isotope ratio peaks from Greenland (Dansgaard *et al.*, 1971) indicative of maximum warming; the glacial readvances (*f*) from New Zealand (Burrows, 1973, 1975), (*g*) from Greenland (Ten Brink & Weidick, 1974), (*h*) from Alaska and (*i*) from Lapland (Denton & Karlén, 1973); (*j*) the Sahara climates (Geyh & Jäkel, 1974) where H denotes humid, and A denotes arid; and (*k*) maximum flood levels of the Nile (Fairbridge, 1962, and pharonic inscriptions). Note that imperfections in the datings exist that might present false impressions of one region 'leading' another.

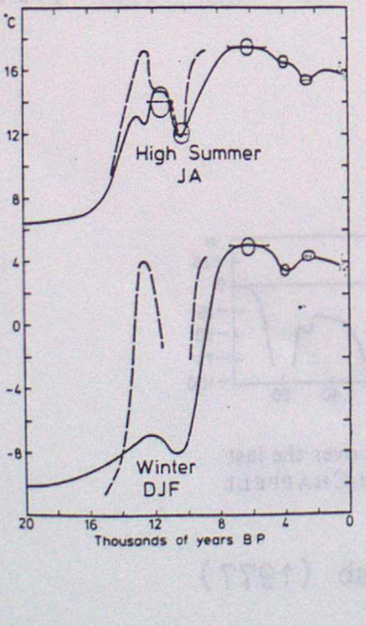

Probable course of prevailing temperatures in central England over the last 20 000 years.

Full lines = mainly from botanical evidence.

Broken lines = amendment suggested by analysis of the beetle fauna.

Ovals = margins of uncertainty of the dating and temperature values derived.

Horizontal bars = apparent duration of the conditions from which the temperature values were derived.

Dots = mean temperature values derived for individual centuries of the last millennium from reported weather or actual temperature measurements (see fig. 6.6, Volume 1, p. 236).

Figure 7.8A From Lamb (1977)

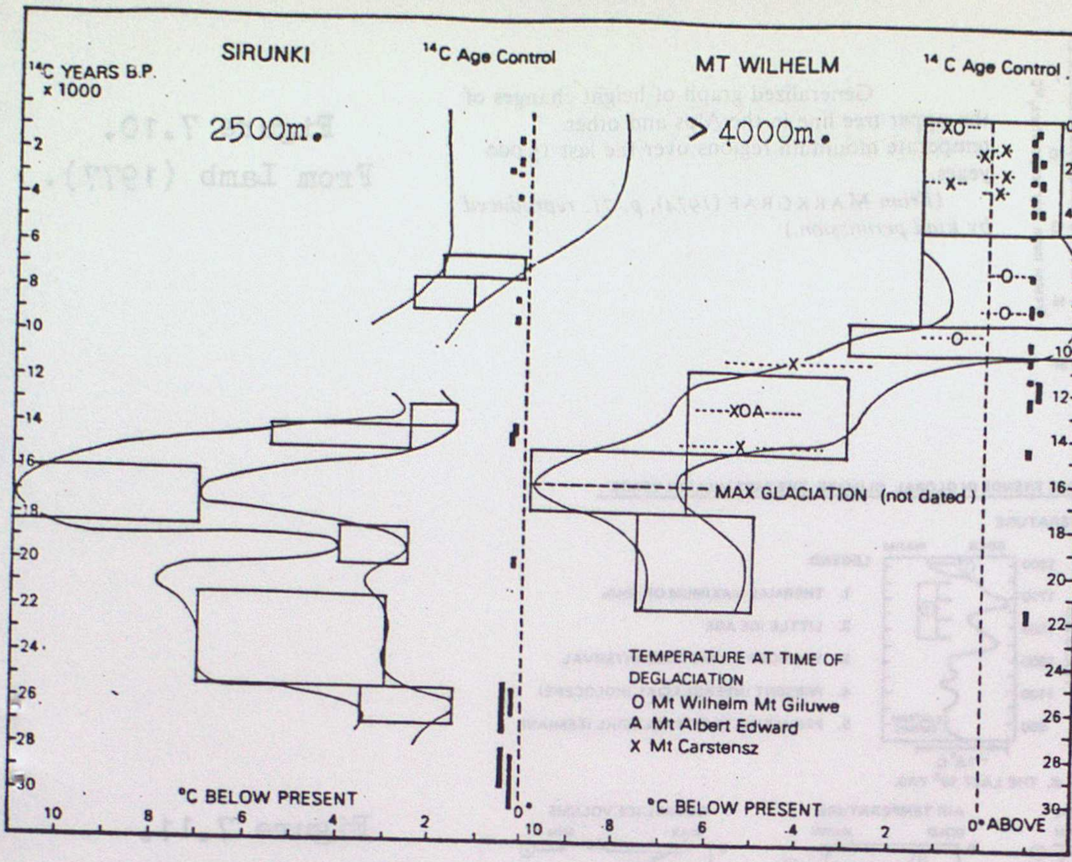

Figure 7.8B. After Bowler et al (1976).

Black rectangles show periods when ^{14}C dates are available.

Limits of temperature variation through the past 28,000 years at two sites in the highlands of New Guinea derived from pollen analysis, with estimates of temperature indicated by glacial stages on four mountains.

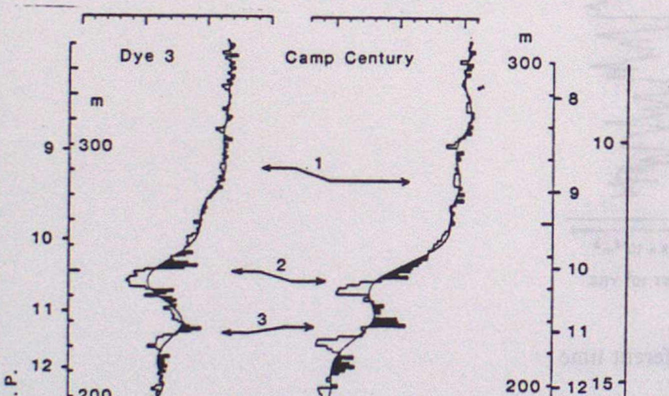

Figure 7.9A. From Dansgaard et al (1982).

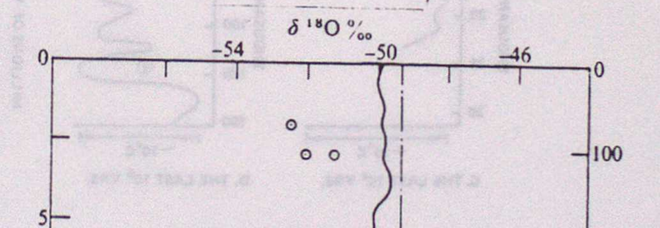

.. Evidence from an Antarctic ice core that the atmospheric CO_2 concentration (dots) was half the present value at the peak of the last glaciation 18000 years ago. The change of ocean volume as the ice melted (15000–10000 years ago) is shown by the change in ^{18}O:^{16}O ratio (continuous curve). (Based on Delmas, Ascencio & Legrand 1980.)

Figure 7.9B.

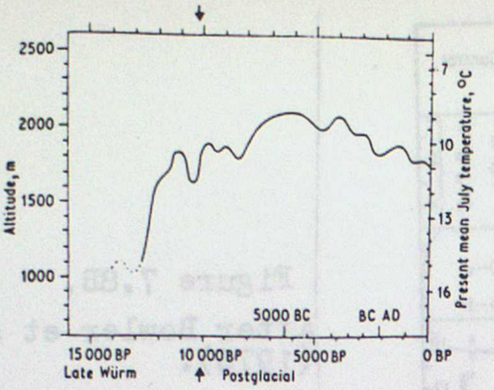

Generalized graph of height changes of the upper tree line in the Alps and other temperate mountain regions over the last 15 000 years.
(*From* MARKGRAF *(1974), p. 71; reproduced by kind permission.)*

Figure 7.10.
From Lamb (1977).

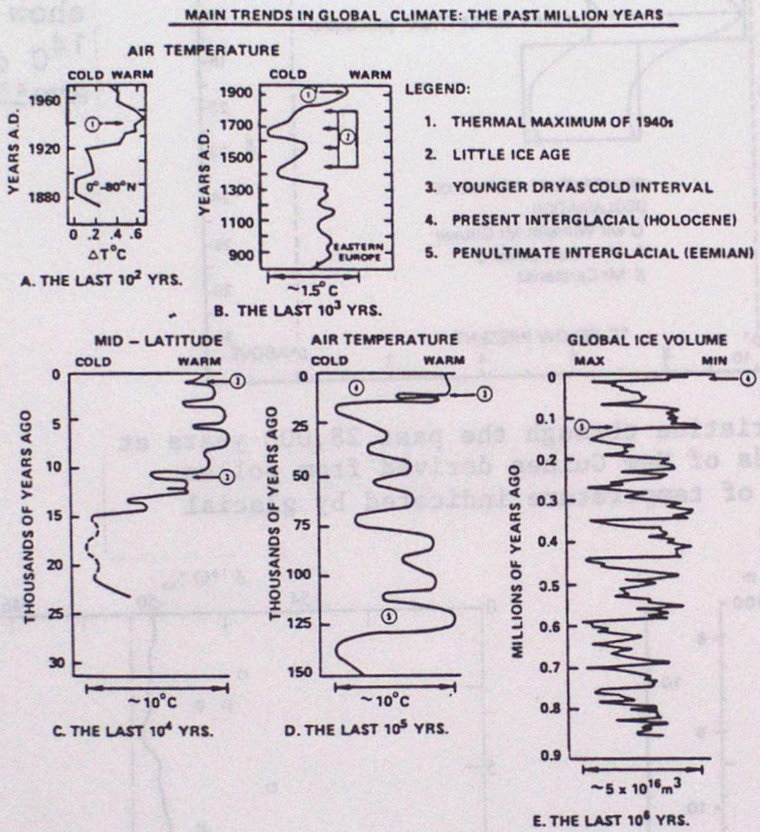

Figure 7.11.

From Lamb (1977).

Indicators of global temperature change: different time spans compared.

(*a*) Successive 5-year mean observed surface air temperatures, last 100 years (MITCHELL *1963*).
(*b*) Winter severity index for Europe near 50°N 35°E, last 1000 years (LAMB *1969*).
(*c*) Generalized temperature changes in middle latitudes of the northern hemisphere, from tree line studies, last 10 000 years (LAMARCHE *1974*).
(*d*) Middle latitudes northern hemisphere air temperature variations, from diagnosis of sea temperatures and from pollen records on land, last 100 000 years (compiled by W. L. GATES from the curves in fig. 15.10).
(*e*) Global ice volume changes from isotope measurements on plankton in a Pacific Ocean sediment core, last million years (as in fig. 15.4).

(Diagram kindly supplied by Drs W. L. GATES *and* J. S. PERRY *with the permission of the U.S. National Academy of Sciences.)*

Figure 7.12A
From Lamb (1977)

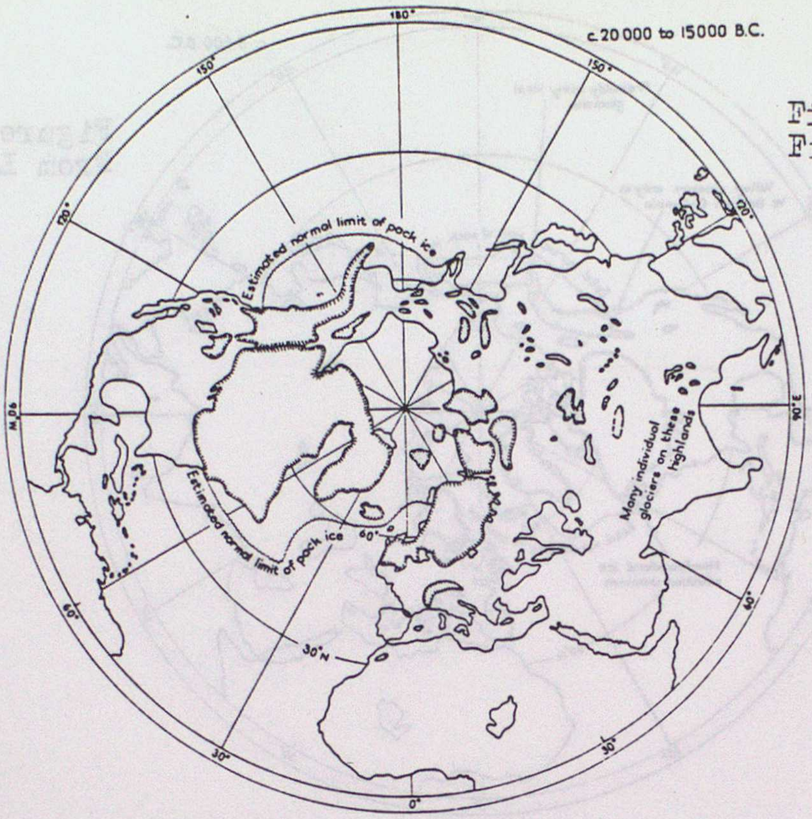

Northern hemisphere geography at the time of the last climax of glaciation about 18 000 years ago.

Figure 7.12B
From Lamb (1977)

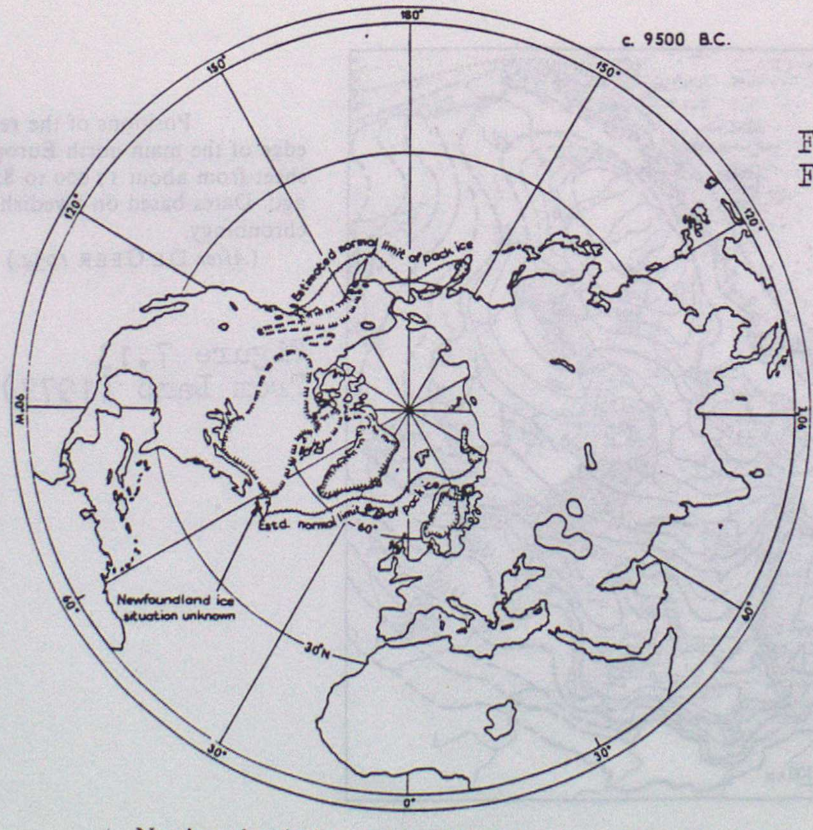

Northern hemisphere geography at the time of the Allerød (warm) interstadial 11 000–12 000 years ago.

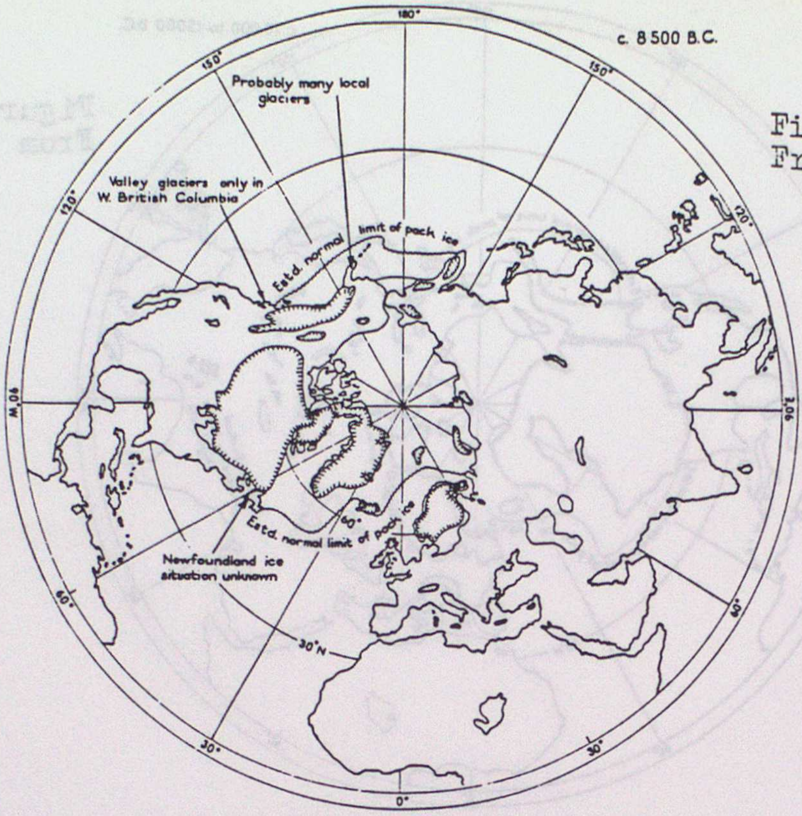

Figure 7.12C
From Lamb (1977)

Northern hemisphere geography during the post-Allerød cold time between about 10 200 and 10 800 years ago.

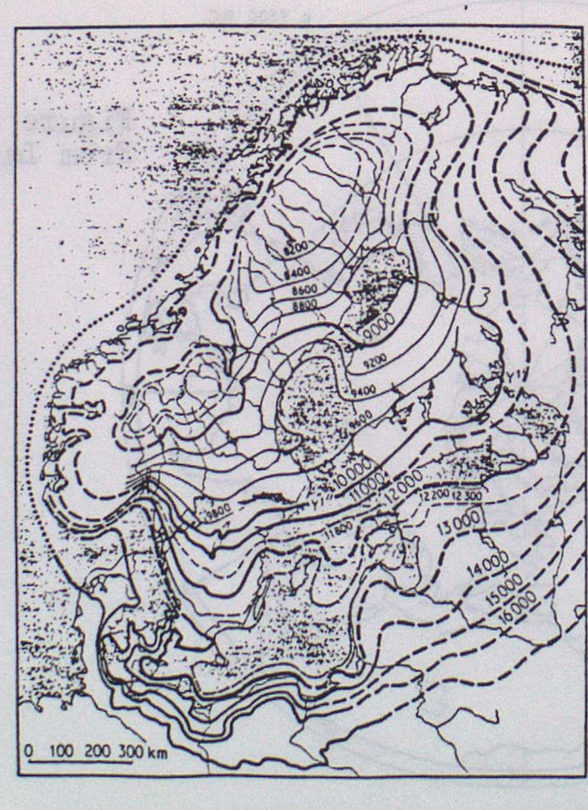

Positions of the retreating edge of the main north European ice sheet from about 17 000 to 8200 years ago. Dates based on Swedish varve chronology.
(*After* DE GEER *1954*.)

Figure 7.13
From Lamb (1977)

A

B

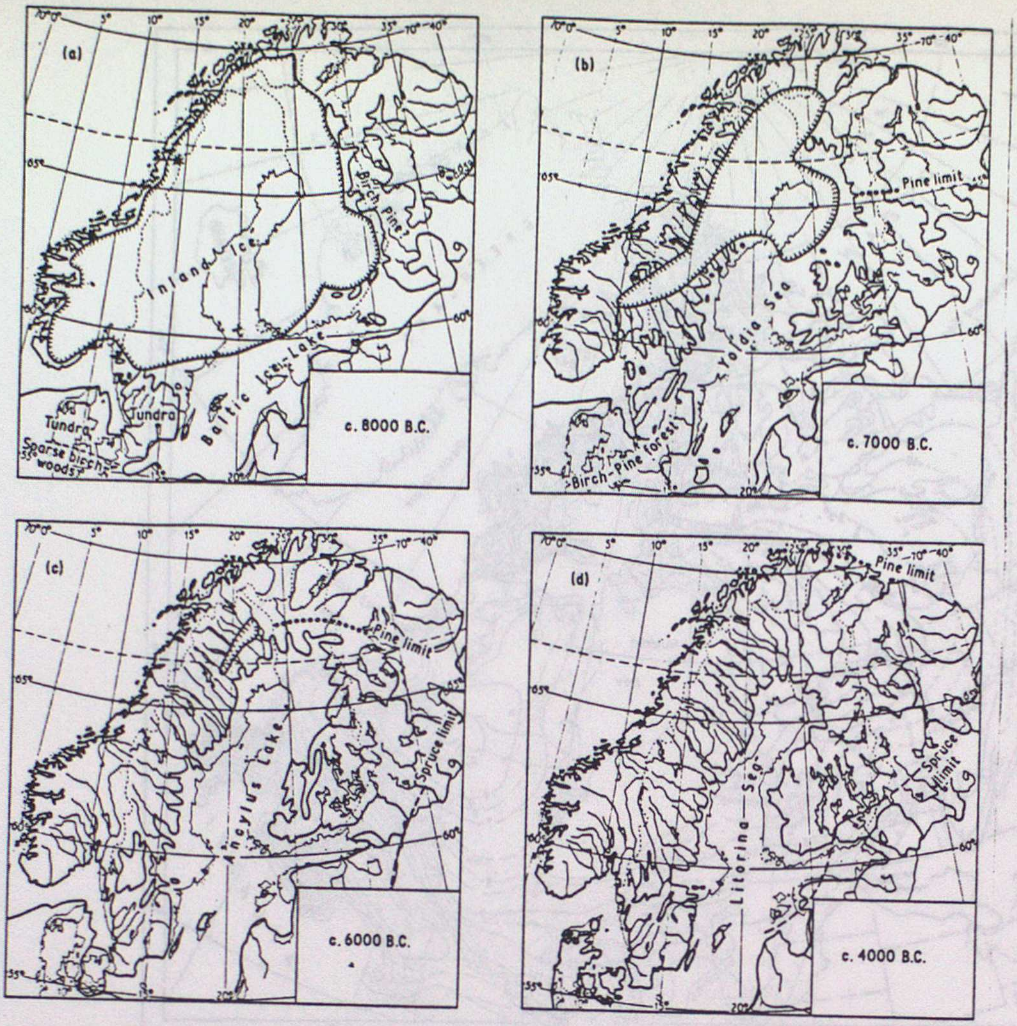

C

D

The postglacial development of the Baltic. (*a*) 8000 B.C. (*b*) 7000 B.C. (*c*) 6000 B.C. (*d*) 4000 B.C.
(*After* HULTÉN *1971*.)

Figure 7.14.
From Lamb (1977).

The geography of Northsealand about 7000 B.C.
(*First published by* CLEMENT REID *in 1902; also in* GODWIN *1956*.)

Figure 7.15.
From Lamb (1977).

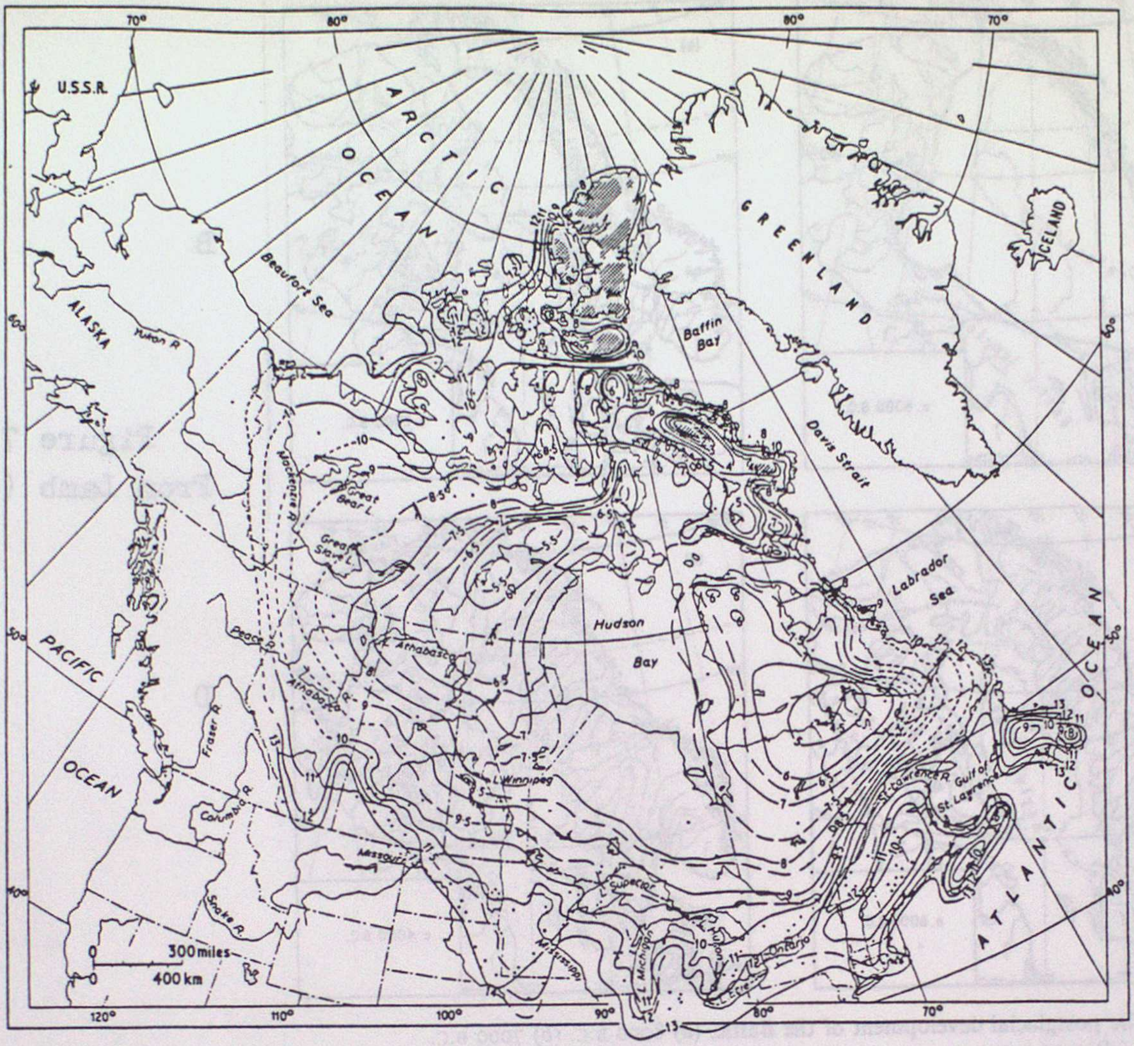

Isochromes of the withdrawal of the North American (Laurentide) ice sheet.
All dates B.P. (before present).
Dots show where radiocarbon dates have been established.
Moraines, coastlines and all other available field evidence used.
(*Reproduced from* BRYSON *et al.* (*1969*); *by kind permission.*)

Figure 7.16 From Lamb (1977)

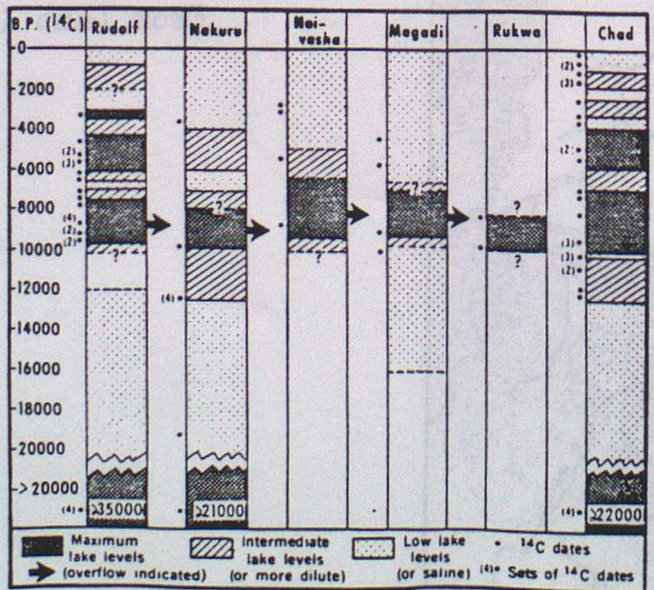

Lake levels in
equatorial and tropical Africa.
Radiocarbon dated high
stands and low stands.

Lake Rudolf (4°30'–2°20'N 35°50'–36°40'E)
Lake Nakuru (0°20'S–36°05'E)
Lake Naivasha (0°50'S 36°20'E)
Lake Magadi (1°55'S 36°15'E)
Lake Rukwa (8°S 32°20'E)
Lake Chad (approx. 13°N 13°E)

(*From* BUTZER *et al. 1972; reproduced by kind permission of the authors and of* Science.)

Figure 7.17 From Lamb (1977)

A

B

C

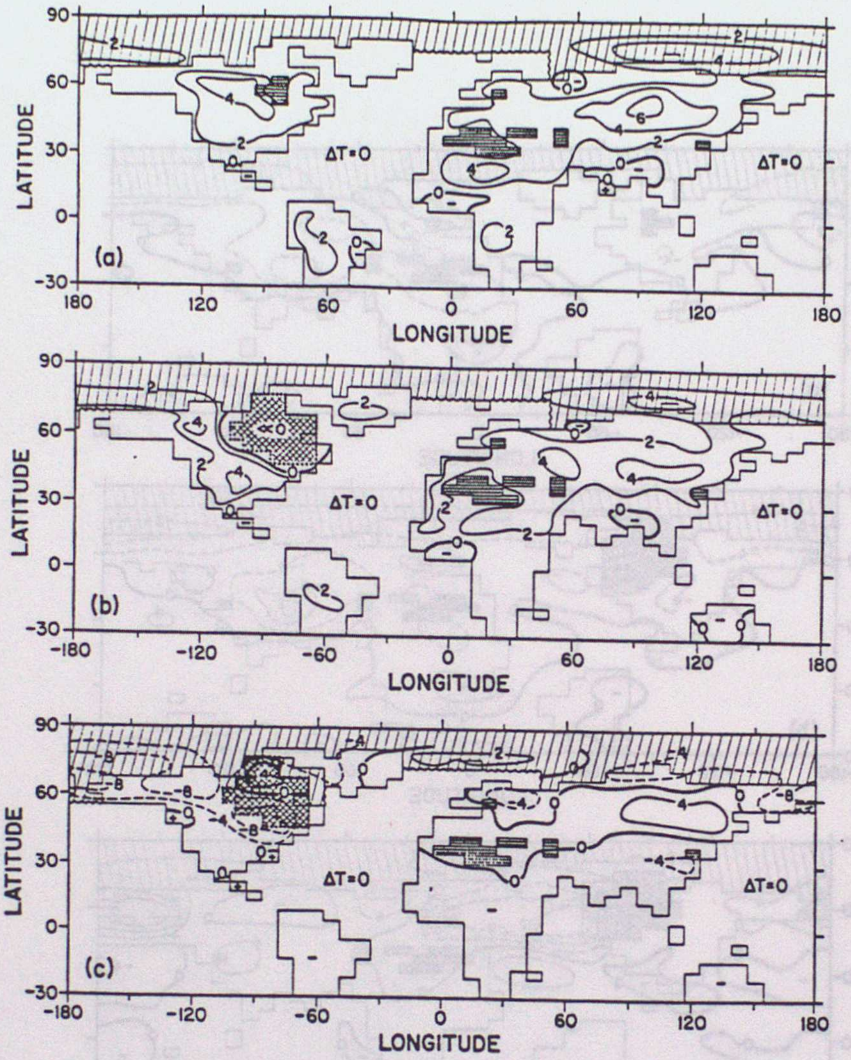

Simulated land surface temperature (K) differences (9 kyr BP minus present) for a) an experiment with solar radiation for July 9 kyr BP, present July ocean surface temperature, and no North American ice sheet ; b) same as (a) except with North American ice-sheet ; c) same as (b) except for January. Temperature difference is prescribed to be zero at ocean gridpoints and at interior sea gridpoints (wavey lines) but not over sea ice (hatched). The area covered by the North American ice sheet is indicated with cross-hatching. Results of the simulation for the region south of 30° s are not shown because the number of land gridpoints is small.

Figure 7.18 From Kutzbach and Guetter (1984)

A

B

C

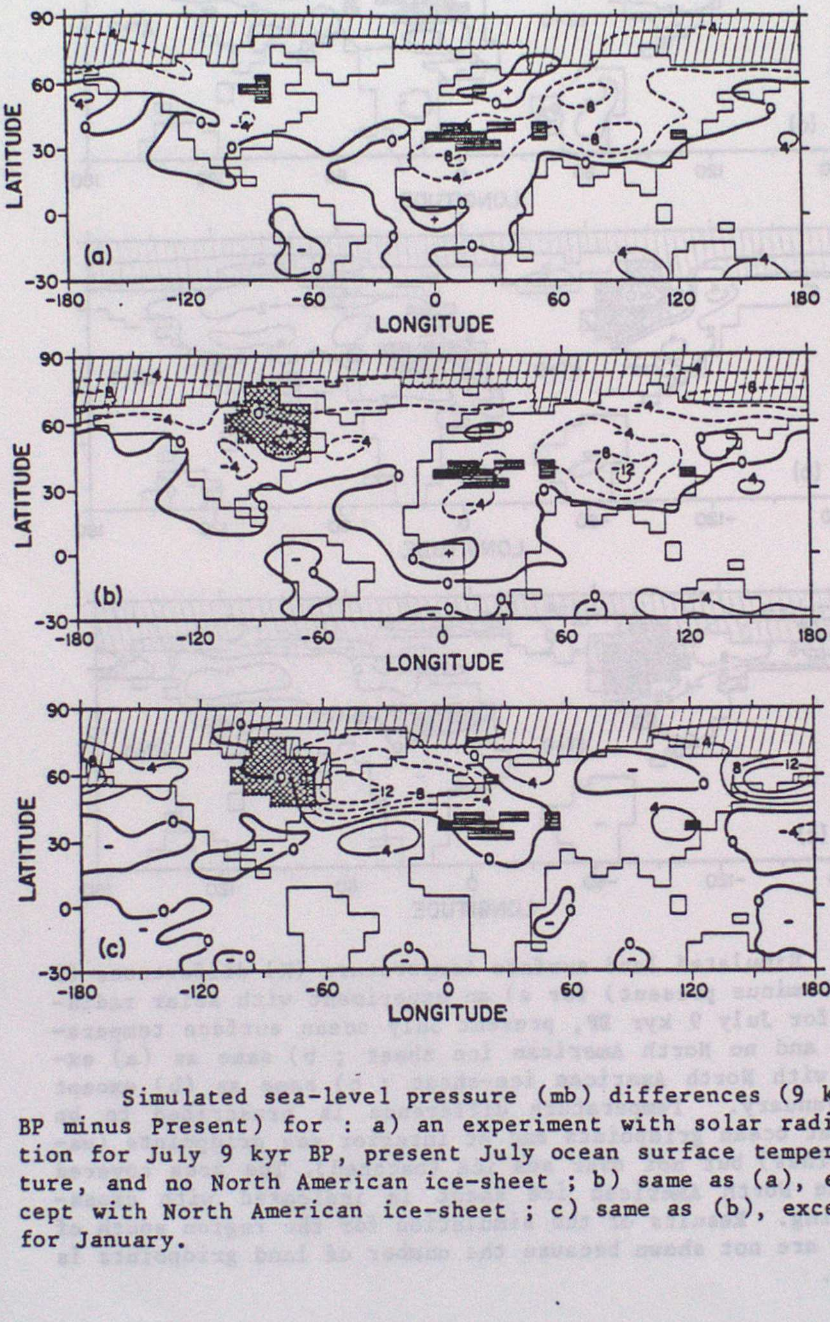

Simulated sea-level pressure (mb) differences (9 kyr BP minus Present) for : a) an experiment with solar radiation for July 9 kyr BP, present July ocean surface temperature, and no North American ice-sheet ; b) same as (a), except with North American ice-sheet ; c) same as (b), except for January.

Figure 7.19 From Kutzbach and Guetter (1984)

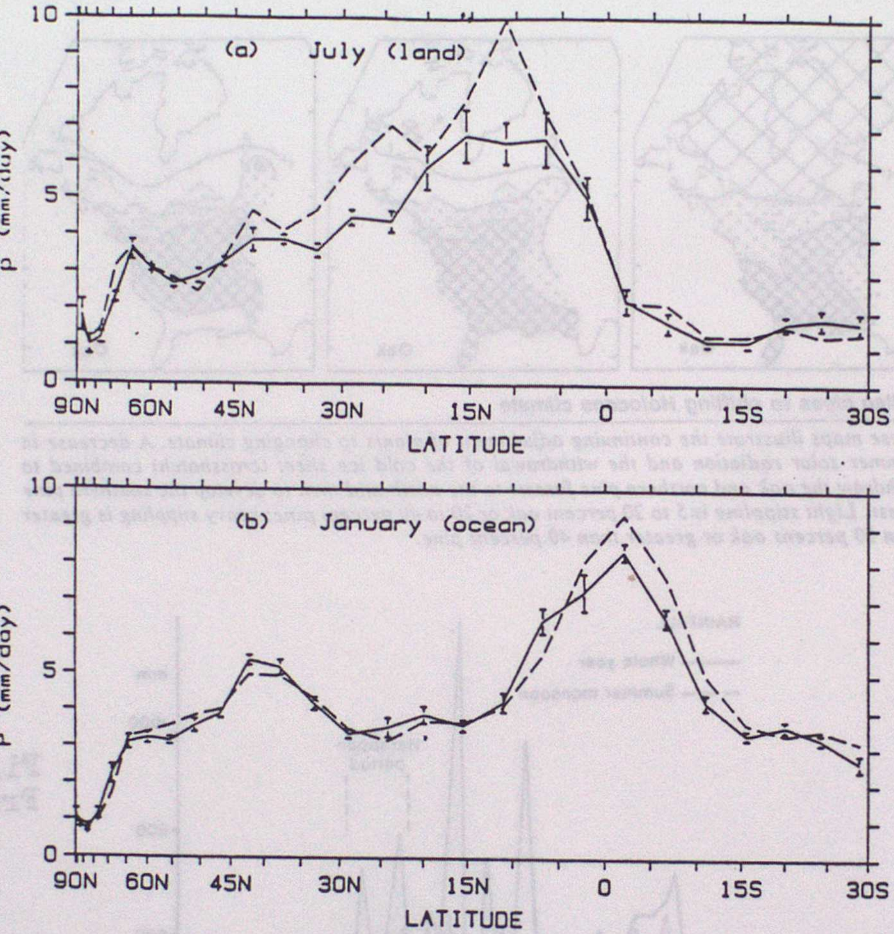

Latitudinal average of simulated precipitation (mm/day) as a function of sine of latitude : a) July—land precipitation; the control simulation (solid line) and the experiment with 9 kyr BP solar radiation and with the North American ice sheet (dashed line) ; b) January—ocean precipitation ; the control simulation (solid line) and the experiment with 9 kyr BP solar radiation and with the North American ice-sheet (dashed line). Vertical bars indicate one standard deviation about the modern control simulation.

Figure 7.20 From Kutzbach and Guetter (1984)

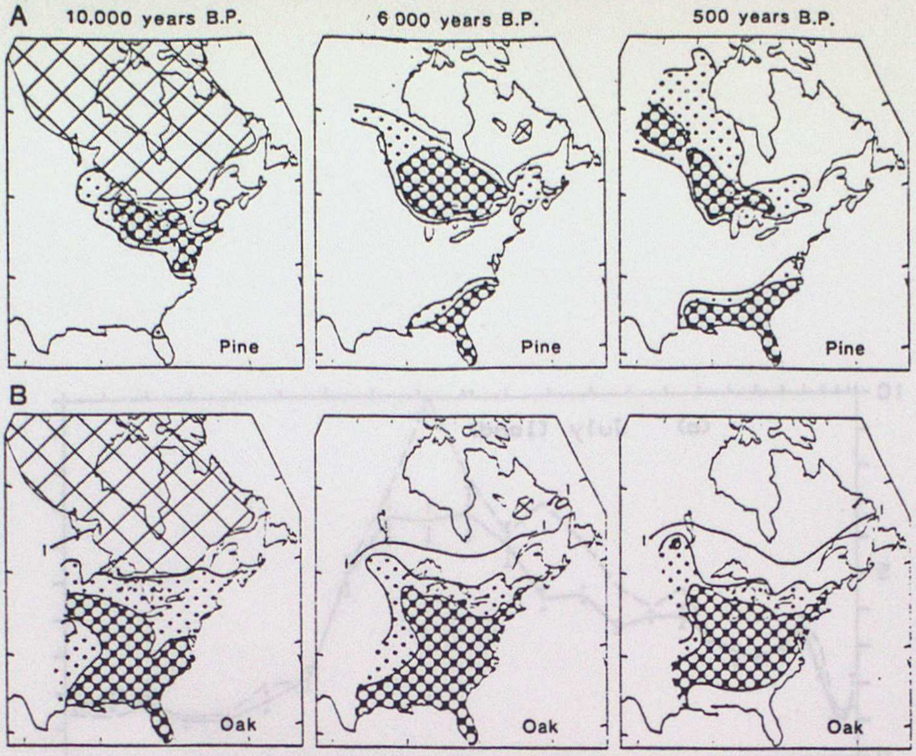

Figure 7.21
From Kerr
(1984)

Pollen clues to shifting Holocene climate

These maps illustrate the continuing adjustment of plants to changing climate. A decrease in summer solar radiation and the withdrawal of the cold ice sheet (crosshatch) combined to withdraw the oak and northern pine forests to the north and then to develop the southern pine forest. Light stippling is 5 to 20 percent oak or 20 to 40 percent pine: heavy stippling is greater than 20 percent oak or greater than 40 percent pine.

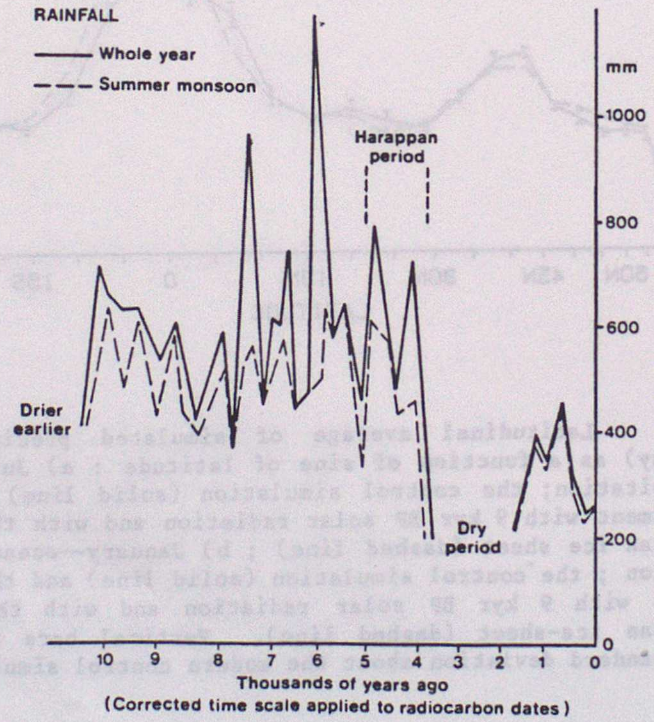

Figure 7.22
From Lamb (1982)

Estimated variations of the rainfall in Rajasthan, northwest India over the last 10,000 years, from lake levels and botanical (pollen analysis) evidence. (Adapted from a diagram by R. A. Bryson, based on the work of G. Singh)

N.B. Figure 7.23 follows Figure 7.25.

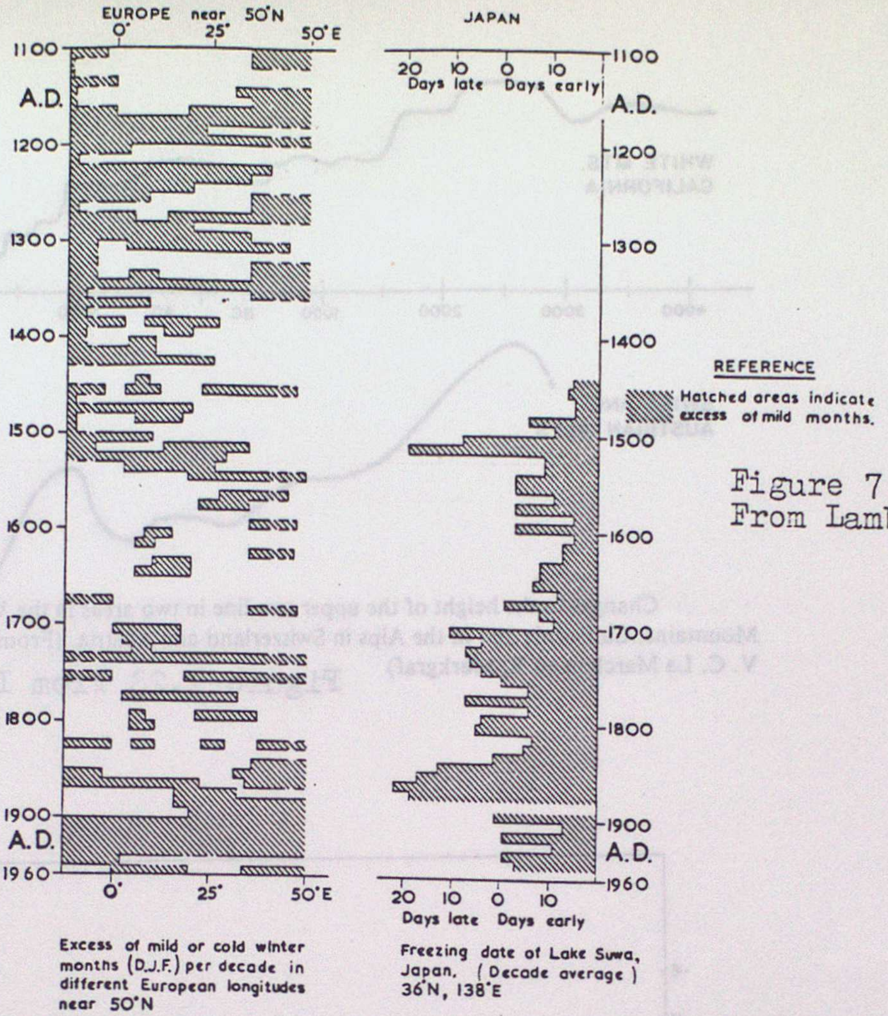

Figure 7.24
From Lamb (1977)

Survey of historical weather records by decades in Europe and Japan.

Left-hand side: Predominance of winter mildness (shaded) or severity (clear) in different European longitudes near 50°N

Right-hand side: Variations of average freezing date of a small lake in central Japan, decade by decade, from the overall mean date.

Europe: decades from A.D. 1100.

Japan: decades from A.D. 1440.

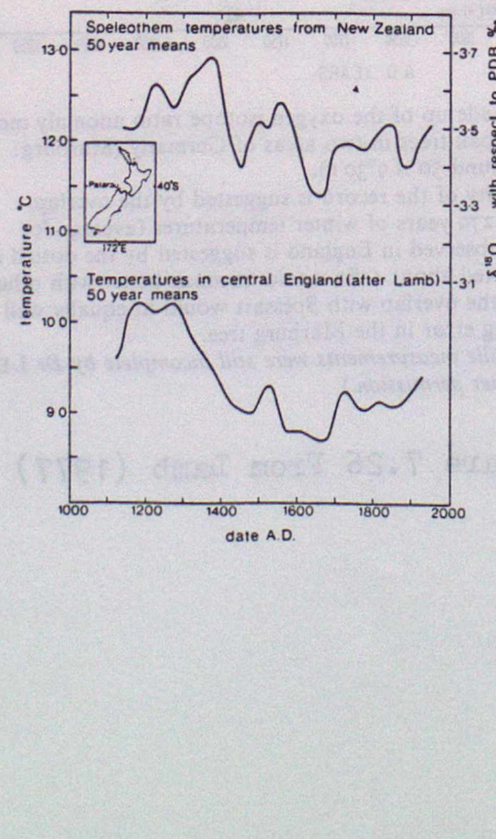

Course of the 50-year mean temperatures in the Nelson area, South Island, New Zealand, since A.D. 1100, derived from oxygen isotope measurements on a stalagmite in a cave at Patarau.

Temperatures derived by LAMB for Central England, as shown in Volume 1, p. 236, are repeated here for comparison.

(Adapted from the original diagram kindly supplied by Professor A. T. WILSON.)

Figure 7.25 From Lamb (1977)

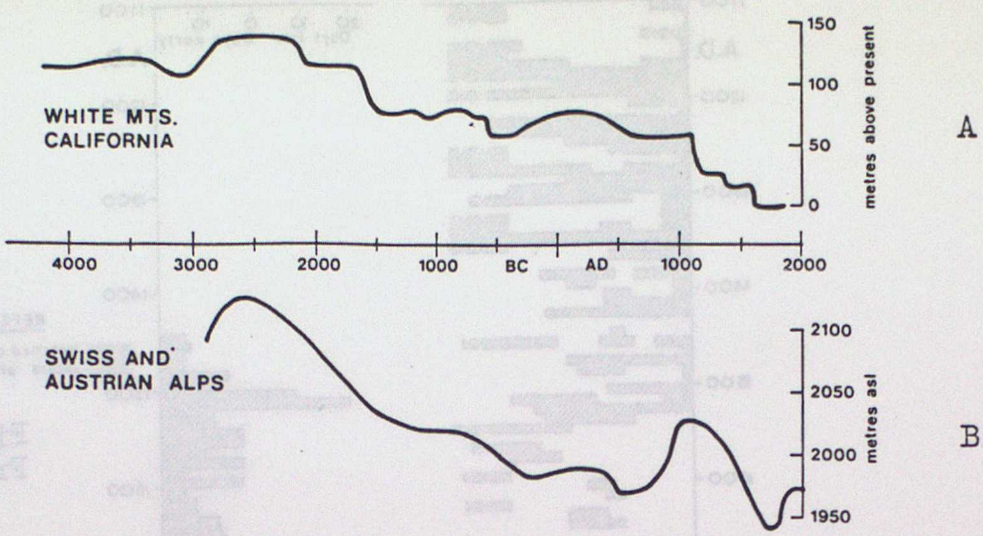

Changes in the height of the upper tree line in two areas in the White Mountains, California and in the Alps in Switzerland and Austria. (From work by V. C. La Marche and V. Markgraf)

Figure 7.23 From Lamb (1982)

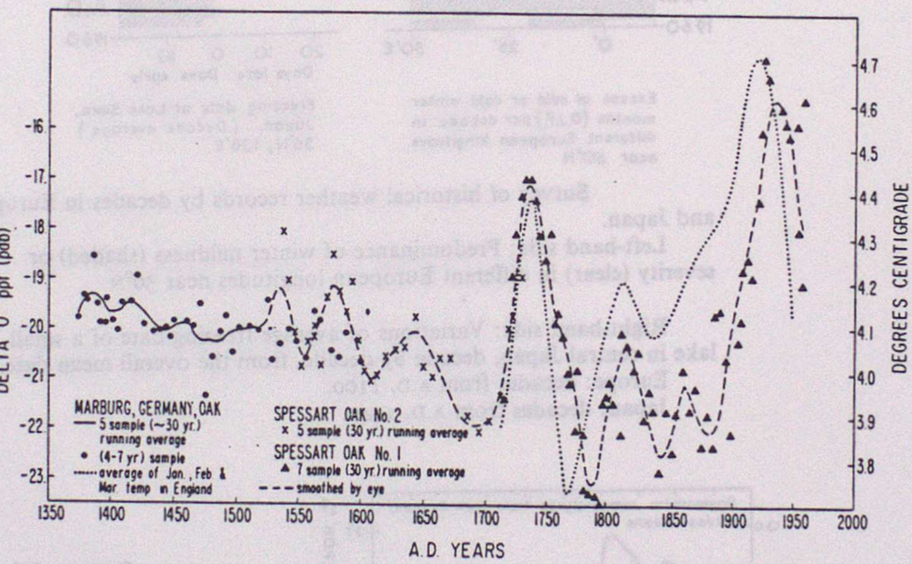

Composite record made up of the oxygen isotope ratio anomaly measured in the (tree-ring-dated) wood of oak trees in two areas of Germany (Marburg: 50°49′N 8°45′E) and Spessart (around 50°N 9°30′E).

Internal consistency/continuity of the record is suggested by the overlap.

Calibration against the last 270 years of winter temperatures (average for January, February and March) observed in England is suggested by the dotted curve.

Note: The very low dot plotted about 1480 would fit much better with other data for the 1430s, and it seems that the overlap with Spessart would fit equally well if there were about a 50-year dating error in the Marburg tree.

(*Diagram kindly provided while measurements were still incomplete by Dr* LEONA M. LIBBY *and reproduced with her permission.*)

Figure 7.26 From Lamb (1977)

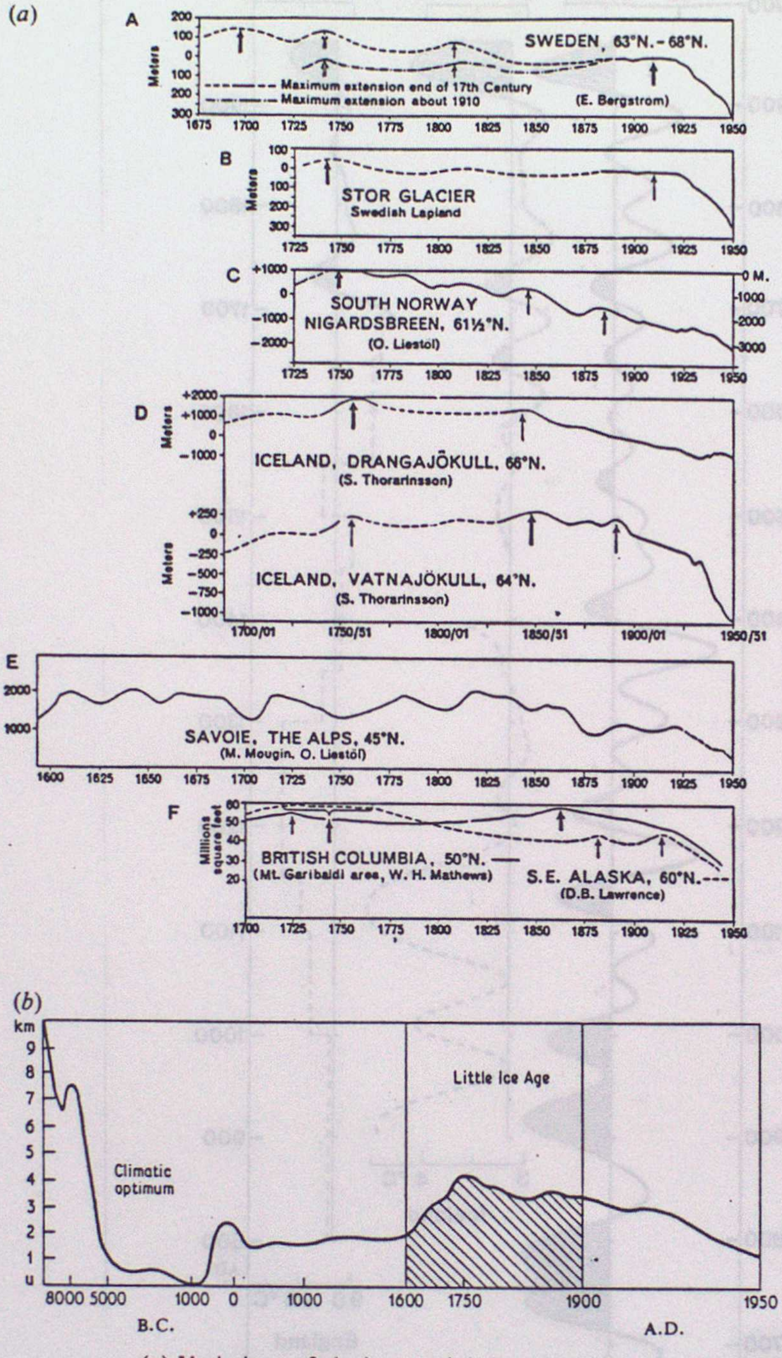

(*a*) Variations of glacier termini since A.D. 1600.
(*b*) Variations in the length in km of the glaciers in Iceland and Norway since 10 000 B.C.
(*After* H. W. AHLMANN *1953*.)

Figure 7.27 From Lamb (1977)

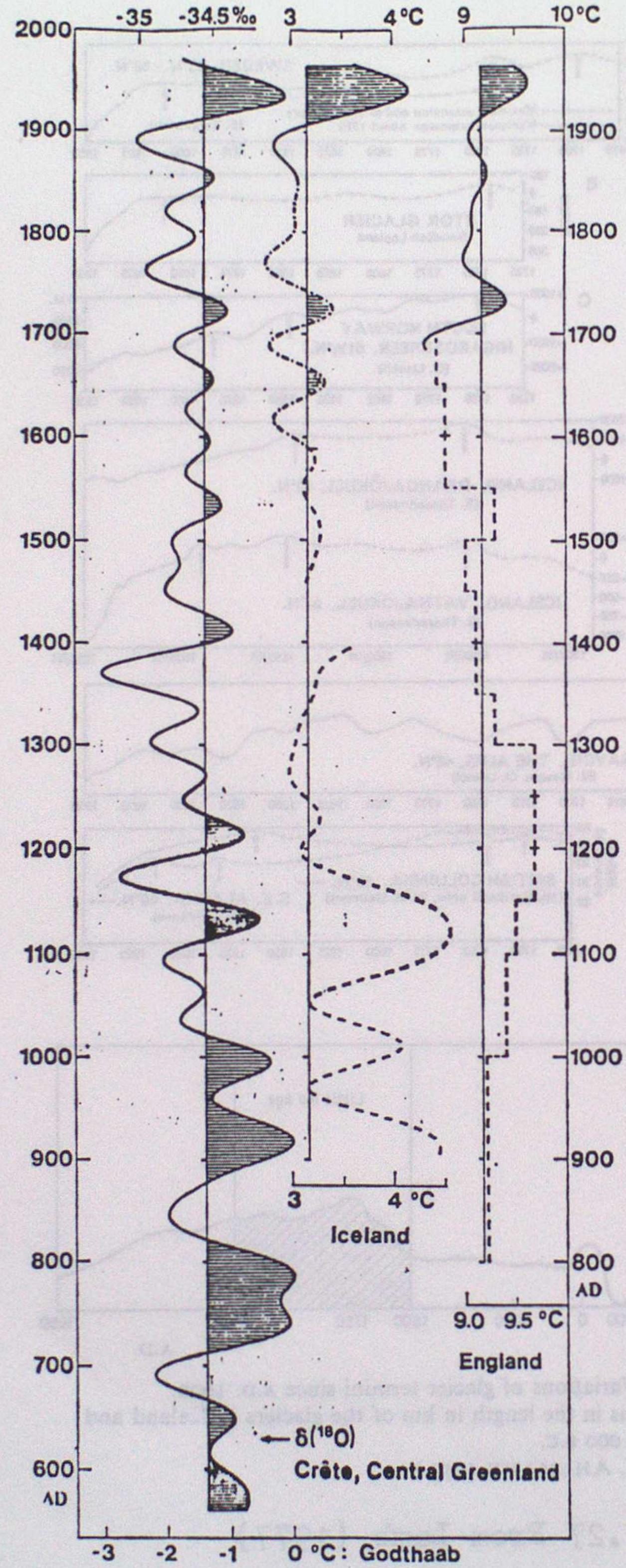

Comparison between the ^{18}O concentration (left) in snow fallen at Crête, Central Greenland, (δ scale on top), and temperatures for Iceland and England. The curves are smoothed by a 60-yr low pass digital filter, except for England 800–1700 AD. The full curves are based on systematic, direct observations, the dashed-dotted part of the Iceland record is estimated from systematic ice observations, whereas the dashed curves depend on indirect evidence.

Figure 7.28 After Dansgaard et al (1975)